Inorg. Chem. **2008**, *47*, 3748−3762

Tuning the Coordination Sphere around Highly Luminescent Lanthanide Complexes

Loïc Charbonnière,*,† Samir Mameri,† Pascal Kadjane,† Carlos Platas-Iglesias,‡ and Raymond Ziessel*,†

Laboratoire de Chimie Moléculaire, associé au CNRS, ECPM-ULP, 25 rue Becquerel, 67087 Strasbourg Cedex 02, France, and Departamento de Química Fundamental, Universidade da Coruña, Campus da Zapateira, Alejandro de la Sota 1, 15008 A Coruña, Spain

Received December 21, 2007

A series of three ligands designed for the formation of water-soluble luminescent lanthanide complexes is described. All ligands are based on a 6″-carboxy-2,2′:6′,2″-terpyridine framework linked via a methylene bridge to *n*-butylamine. The second negatively charged arm consists of a 6-carboxy-2-methylenepyridine for **L1**, a 6′-carboxy-6-methylene-2,2′-bipyridine for **L2**, and a 6″-carboxy-6-methylene-2,2′:6′,2″-terpyridine for **L3**. The photophysical properties of the Eu and Tb complexes were studied in aqueous solutions by means of absorption spectroscopy and steady-state and time-resolved luminescence spectroscopy. Luminescence excited-state lifetimes were recorded and led to the determination of two water molecules in the first coordination sphere. The europium complexes were characterized by means of ^{1}H NMR spectroscopy in D_2O and DFT calculations performed at the B3LYP level both in vacuo and in aqueous solution. Finally, the influence of different phosphorylated anions such as HPO_4^{2-}, ATP^{4-}, ADP^{3-}, and AMP^{2-} on the luminescence properties of the $[Eu\mathbf{L}\boldsymbol{X}(H_2O)_2]^+$ complexes ($X = 1-3$) was investigated in buffered aqueous solutions (0.01 M TRIS, pH 7.0), showing a significant interaction of ATP^{4-} with $[Eu(\mathbf{L2})(H_2O)_2]^+$. The coordination of anions was understood in terms of partial decomplexation of one arm of the ligands and water displacement, with formation of ternary species, and it was rationalized on the basis of the structural models of the complexes obtained from DFT calculations.

Introduction

The coordination chemistry of lanthanide complexes appears as a particular field of its own along the periodic table. The shielding of the 4f shell by external filled orbitals almost prevents the participation of these valence electrons in covalent interactions, and the resulting lack of stereoelectronic preferences prevents a strict rationalization of the ligand design through well-defined geometrical rules. However, the very broad scope of electronic, spectroscopic, or isotopic properties of this series of elements offers so much potential that their coordination has triggered an enormous interest in the scientific community. In particular, the presence of unpaired electrons confers them paramagnetic properties[1] used for structural determination in solution[2] or for the development of contrast agents in nuclear magnetic resonance imaging,[3] while a large variety of radioactive isotopes of lanthanide complexes can be used in nuclear medicine for both diagnosis and therapy.[4] Finally the sharp and characteristic emission spectra of some luminescent

* To whom correspondence should be addressed. Tel.: (33) 3 90 24 26 90. Fax: (33) 3 90 24 27 42. E-mail: l.charbonn@chimie.u-strasbg.fr (L.C.).
† ECPM-ULP.
‡ Universidade da Coruña.

(1) (a) Reilley, C. N.; Good, B. W.; Desreux, J. F. *Anal. Chem.* **1975**, *47*, 2110–2115. (b) Bertini, I.; Turano, P.; Vila, A. J. *Chem. Rev.* **1993**, *93*, 2833–2932.
(2) (a) Forsberg, J. H. In *Handbook on the Physics and Chemistry of Rare Earths*; Gschneider, K. A., Eyring, L., Eds.; Elsevier: Amsterdam, 1996; Vol. *23*, Chapter 153, pp 1–68. (b) Piguet, C.; Geraldes, C. F. G. C. In *Handbook on the Physics and Chemistry of Rare Earths*; Gschneider, K. A., Bünzli, J.-C. G., Pecharsky, V. K., Eds.; Elsevier: Amsterdam, 2003; Vol. *33*, pp 353–463.
(3) (a) Toth, E.; Helm, L.; Merbach, A. E. In *The Chemistry of Contrast Agents in Medical Magnetic Resonance Imaging*; Merbach, A. E., Toth, E., Eds.; Wiley: Chichester, U.K., 2001; pp 45–119. (b) Caravan, P.; Ellison, J. J.; McMurry, T. J.; Lauffer, R. B. *Chem. Rev.* **1999**, *99*, 2293–2352.
(4) (a) Nayak, D.; Lahiri, S. *J. Radioanal. Nucl. Chem.* **1999**, *242*, 423–432. (b) Kaden, T. A. *Dalton Trans.* **2006**, 3617–3623.

10.1021/ic702472n CCC: $40.75
Published on Web 04/05/2008

lanthanide complexes offer great perspectives for cellular imaging[5] and for highly sensitive fluoro-immunoassays.[6]

However, whatever the targeted application, the use of lanthanide complexes requires some stringent prerequisites to maintain their integrity in aqueous solutions and even more in highly competitive biological media (blood, sera). Water-stable lanthanide complexes are generally obtained from macrocyclic ligands based on branched tetraazacyclododecane,[7] triazacyclononane,[8] and other cycles,[9] on podand type structures[10] potentially based on supramolecular preorganization,[11] or on elaborated cryptand-like macrobicyclic architectures.[12] In most cases, the water stability is achieved by the introduction of anionic functions such as acetate arms, which provides strong electrostatic interactions with the triply charged lanthanide cations. In the particular case of luminescent lanthanide complexes,[13] the ligand should provide the following features: (i) protecting the Ln from water molecules and their associated nonradiative deactivation pathways,[14] (ii) generating an antenna effect for an efficient sensitization of the Ln,[15,16] and (iii) providing a molecular pocket in which stability is ensured by charge compensation.

An efficient synthetic approach to obtain sensitizing ligands is to introduce the absorbing units as coordinating units of the ligand. Apart from the case of cryptand molecules,[12] the presence of anionic functions such as carboxylate and phosphonate anions normally ensures a high thermodynamic stability in water. Along these lines, numerous efforts have been devoted to the introduction of polyaminocarboxylate functions on heteroaromatic platforms,[13,17] while only a few examples are based on the polyheteroaromatic ligands containing these functions as part of the aromatic frameworks. The simplest example, 6-carboxypyridine, have been shown to be easily introduced on elaborated preorganized structures such as podand type structures[8a,18] or a simpler ethylenediamine bridge,[19] while dipicolinic acid is known to be an excellent coordinating ligand, either on its own[20] or introduced as a binding unit in more elaborated ligands.[21] Unfortunately, a single pyridine ring only affords excitation in the far-UV region around 270–280 nm,[19] which negates its use for applications in biological media in which aromatic amino acids and nucleotides would absorb most of the excitation light. It is thus of interest to target extended polyaromatic structures that absorb at lower energies. Within this context, the symmetrical 6,6′-dicarboxy-2,2′-bipyridine[22,23] and derivatives of 2,9-dicarboxy-1,10-phenanthroline[23,24] proved to be good sensitizers for Ln emission. Asymmetrically substituted ligands based on various anionic biaromatic frames such as benzimidazolylpyridinecarboxylate,[11a,25] 2-carboxy-1,10-phenanthroline,[26] 6-carboxy-2-pyrazolylpyridine,[27] and 6-carboxy-2,2′-bipyridine[8b,26,28,29] have also been adequately used as chelating antennas. They present an excitation domain around 300–320 nm and display convenient photosensitization efficiencies[30] and good thermodynamic stabilities when incorporated into preorganized frameworks.[8b] A

(5) (a) Seveus, L.; Väisälä, M.; Syrjänen, S.; Sandberg, M.; Kuusisto, A.; Harju, R.; Salo, J.; Hemmilä, I.; Kojola, H.; Soini, E. *Cytometry* **1992**, *13*, 329–338. (b) Yu, J.; Parker, D.; Pal, R.; Poole, R. A.; Cann, M. J. *J. Am. Chem. Soc.* **2006**, *128*, 2294–2299.

(6) (a) Hemmilä, I.; Mukala, V.-M. *Crit. Rev. Clin. Lab. Sci.* **2001**, *38*, 441–519. (b) Hildebrandt, N.; Charbonnière, L.; Beck, M.; Ziessel, R. F.; Löhmannsröben, H.-G. *Angew. Chem., Int. Ed.* **2005**, *44*, 7612–7615. (c) Yuan, J.; Wang, G. *J. Fluorescence* **2005**, *15*, 559–568.

(7) Kumar, K.; Chang, C. A.; Francesconi, L. C.; Dischino, D. D.; Malley, M. F.; Gougoutas, J. Z.; Tweedle, M. F. *Inorg. Chem.* **1994**, *33*, 3567–3575.

(8) (a) Takkalo, H.; Hemmilä, I.; Sutela, T.; Latva, M. *Helv. Chim. Acta* **1996**, *79*, 789–802. (b) Charbonnière, L.; Ziessel, R.; Guardigli, M.; Roda, A.; Sabbatini, N.; Cesario, M. *J. Am. Chem. Soc.* **2001**, *123*, 2436–2437. (c) Tei, L.; Blake, A. J.; Wilson, C.; Schröder, M. *Dalton Trans.* **2004**, 1945–1952.

(9) Bluhm, M. E.; Hay, B. P.; Kim, S. S.; Dertz, E. A.; Raymond, K. N. *Inorg. Chem.* **2002**, *41*, 5475–5478.

(10) (a) Senegas, J.-M.; Bernardinelli, G.; Imbert, D.; Bünzli, J.-C. G.; Morgantini, P.-Y.; Weber, J.; Piguet, C. *Inorg. Chem.* **2003**, *42*, 4680–4695. (b) Weibel, N.; Charbonnière, L.; Ziessel, R. *Tetrahedron Lett.* **2006**, *47*, 1793–1796.

(11) Lessmann, J. J.; Horrocks, W. D. W., Jr. *Inorg. Chem.* **2000**, *39*, 3114–3124.

(12) (a) Alpha, B.; Lehn, J.-M.; Mathis, G. *Angew. Chem., Int. Ed.* **1987**, *26*, 266–269. (b) Galaup, C.; Azéma, J.; Tisnès, P.; Picard, C.; Ramos, P.; Juanes, O.; Brunet, E.; Rodrigues-Ubis, J. C. *Helv. Chim. Acta* **2002**, *85*, 1613–1625.

(13) (a) Bünzli, J.-C. G.; Piguet, C. *Chem. Soc. Rev.* **2005**, *34*, 1048–1077. (b) Brunet, E.; Juanes, O.; Rodrigez-Ubis, J. C. *Curr. Chem. Biol.* **2007**, *1*, 11–39. (c) Bünzli, J.-C. G. *Acc. Chem. Res.* **2006**, *39*, 53–61.

(14) (a) Supkowski, R. M.; Horrocks, W. D. W., Jr. *Inorg. Chim. Acta* **2002**, *340*, 44–48. (b) Horrocks, W. D. W., Jr.; Sudnick, D. R. *J. Am. Chem. Soc.* **1979**, *101*, 334–340. (c) Beeby, A.; Clarkson, I. M.; Dickins, R. S.; Faulkner, S.; Parker, D.; Royle, L.; de Sousa, A. S.; Williams, J. A. G.; Woods, M. *J. Chem. Soc., Perkin Trans. 2* **1999**, 493–503. (d) Stein, G.; Würzberg, E. *J. Chem. Phys.* **1975**, *62*, 208–213. (e) Kimura, T.; Kato, Y. *J. Alloys Compd.* **1998**, *275*, 806–810.

(15) Weissman, S. I. *J. Chem. Phys.* **1942**, *10*, 214.

(16) Sabbatini, N.; Guardigli, M.; Lehn, J.-M. *Coord. Chem. Rev.* **1993**, *123*, 201–228.

(17) (a) Yuan, J.; Wang, G. *Trends Anal. Chem.* **2006**, *25*, 490–500. (b) Pandya, S.; Yu, J.; Parker, D. *Dalton Trans.* **2006**, 2757–2766. (c) Yam, V. W.-W.; Lo, K. K.-W. *Coord. Chem. Rev.* **1998**, *184*, 157–240.

(18) (a) Mato-Iglesias, M.; Platas-Iglesias, C.; Djanashvili, K.; Peters, J. A.; Toth, E.; Balogh, E.; Müller, R. N.; van der Elst, L.; de Blas, A.; Rodriguez-Blas, T. *Chem. Commun.* **2005**, 4729–4731. (b) Mato-Iglesias, M.; Balogh, E.; Platas-Iglesias, C.; de Blas, A.; Rodriguez-Blas, T. *Dalton Trans.* **2006**, 5404–5415. (c) Weibel, N.; Charbonnière, L.; Ziessel, R. *Tetrahedron Lett.* **2006**, *47*, 1793–1796. (d) Bretonnière, Y.; Mazzanti, M.; Pécaut, J.; Dunand, F. A.; Merbach, A. E. *Inorg. Chem.* **2001**, *40*, 6737–6745.

(19) Chatterton, N.; Bretonnière, Y.; Pécaut, J.; Mazzanti, M. *Angew. Chem., Int. Ed.* **2005**, *117*, 7767–7770.

(20) (a) Brayshaw, P. A.; Bünzli, J.-C. G.; Froidevaux, P.; Harrowfield, J. M.; Kim, Y.; Sobolev, A. N. *Inorg. Chem.* **1995**, *34*, 2068–2076. (b) Chauvin, A.-S.; Gumy, F.; Imbert, D.; Bünzli, J.-C. G. *Spectrosc. Lett.* **2004**, *37*, 517–532. (c) Ouali, N.; Bocquet, B.; Rigault, S.; Morgantini, P.-Y.; Weber, J.; Piguet, C. *Inorg. Chem.* **2002**, *41*, 1436–1445. (d) Platas-Iglesias, C.; Piguet, C.; André, N.; Bünzli, J.-C. G. *Dalton Trans.* **2001**, 3084–3091.

(21) (a) Senegas, J.-M.; Bernardinelli, G.; Imbert, D.; Bünzli, J.-C. G.; Morgantini, P.-Y.; Weber, J.; Piguet, C. *Inorg. Chem.* **2003**, *42*, 4680–4695.

(22) (a) Mukkala, V.-M.; Kwiatkowski, M.; Kanakare, J.; Takalo, H. *Helv. Chim. Acta* **1993**, *76*, 893–899. (b) Bünzli, J.-C. G.; Charbonnière, L.; Ziessel, R. F. *Dalton Trans.* **2000**, 1917–1923.

(23) Sammes, P. G.; Shek, L.; Watmore, D. *Chem. Commun.* **2000**, 1625–1626.

(24) Evangelista, R. A.; Pollak, A.; Allore, B.; Templeton, E. F.; Morton, R. C.; Diamandis, E. P. *Clin. Biochem.* **1988**, *21*, 173–178.

(25) Elhabiri, M.; Scopelliti, R.; Bünzli, J.-C. G.; Piguet, C. *Chem. Commun.* **1998**, 2347–2348.

(26) Ziessel, R.; Weibel, N.; Charbonnière, L. J. *Synthesis* **2006**, *18*, 3127–3133.

(27) (a) Charbonnière, L. J.; Ziessel, R. *Helv. Chim. Acta* **2003**, *86*, 3402–3410. (b) Charbonnière, L. J.; Ziessel, R. *Tetrahedron Lett.* **2003**, *44*, 6305–6307.

Scheme 1. Principle of Sequential Competitive Binding of Anions

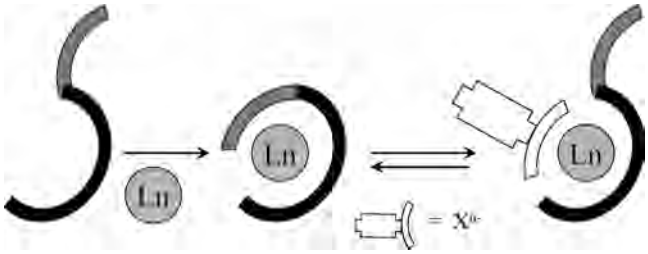

Chart 1

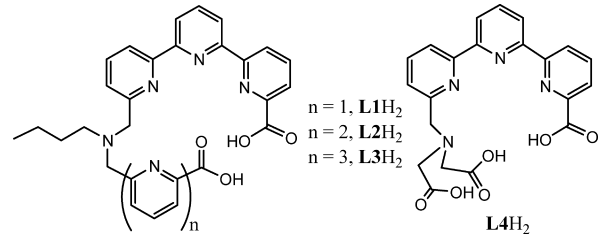

further displacement of the excitation wavelength toward the visible region can be achieved with tris-heteroaromatic scaffolds, but only very few of them possess anionic functions directly linked to the aromatic rings.[31,32]

As a consequence of their peculiar photophysical properties, lanthanide complexes have been widely studied within the framework of luminescent probes for anion detection.[33] They can be used directly as monitors of the luminescence changes,[34] as ratiometric probes,[35] where the relative intensities of the f−f transitions change upon anion coordination, or as time-resolved probes,[36] in which the interaction with anions induces changes in the luminescence lifetime of the complexes. In previous works in this field, we demonstrated that efficient anion detection can be achieved by taking advantage of the *sequential competitive binding* concept. The large coordination numbers of lanthanide complexes in solution, typically 8 to 10, are particularly well suited for this process, depicted in Scheme 1. The principle is based on the design of ligands having heterotopic coordination sites with very different coordination strengths. In the absence of competing anions, the different appended arms are ligated to the Ln cation. The introduction of a competing anion results in the sequential decomplexation of one arm according to its coordination strengths, with formation of a ternary adduct. Importantly, the second arm has to remain tightly coordinated to the cation in order to avoid irreversible decomplexation.

We previously demonstrated that some bis-bipyridine phosphine oxide complexes of Eu and Tb function as anion probes in organic solutions[37] and that additions of anions such as F^-, Cl^-, NO_3^-, and CH_3COO^- resulted in the successive decomplexation of the bipyridyl arms. Considering the known affinity of Ln cations for phosphorylated species[38] and the importance of phosphorylated species and phosphorylation processes in biological phenomena,[39] we also turned our attention toward the detection of phosphorylated nucleosides (nucleotides). In an effort to obtain water-soluble anion sensors, ligands bearing carboxylate functions were designed.[40,41] The corresponding complexes were efficiently able to report the presence of different anions, in particular phosphorylated anions such as ADP^{3-}, ATP^{4-}, and HPO_4^{2-}. Replacing a bipyridine strand by a terpyridine one, as in **L1**−**L3** (Chart 1), is expected to provide very stable complexes, while maintaining the possibility of competitive sequential binding.

In an effort to understand the structure–activity relationship associated with the family of anionically substituted poly-heteroaromatic frameworks, we designed the series of three new ligands **L1**−**L3** (Chart 1), based on a 6-carboxy-2,2′:6′,2″-terpyridine coordinating arm, linked by a methylene bridge to an *n*-butylamine function and a third pyridine-, bipyridine-, or terpyridynecarboxylate arm. The systematic study of the effect of the number of pyridine rings on the coordination properties is expected to highlight the relative coordinating strengths of the different arms and to emphasize the parameters allowing a possible sequential decoordination in the presence of competing anions. The coordination behavior toward Eu and Tb was investigated by means of various spectroscopic techniques, and the influence of phosphorylated anions such as AMP^{2-}, ADP^{3-}, ATP^{4-}, and phosphate on the luminescence properties of the Eu complexes is presented. Density functional theory (DFT) calculations performed both in vacuo and in aqueous solution are used to obtain information about the structure of the complexes in solution, as well as to rationalize their anion recognition ability. When necessary, the ligand $\mathbf{L4}H_2$, containing only the terpyridine core and its Ln complexes,[32b] will be used as reference.

(28) (a) Weibel, N.; Charbonnière, L. J.; Guardigli, M.; Roda, A.; Ziessel, R. *J. Am. Chem. Soc.* **2004**, *126*, 4888–4896. (b) Charbonnière, L. J.; Weibel, N.; Retailleau, P.; Ziessel, R. *Chem. Eur. J.* **2007**, *13*, 346–358. (c) Ziessel, R. F.; Charbonnière, L. J.; Cesario, M.; Prangé, T.; Guardigli, M.; Roda, A.; van Dorselaer, A.; Nierengarten, H. *J. Supramol. Chem.* **2003**, *15*, 277–289. (d) Charbonnière, L. J.; Weibel, N.; Ziessel, R. F. *J. Org. Chem.* **2002**, *67*, 3933–3936. (e) Charbonnière, L. J.; Weibel, N.; Ziessel, R. F. *Synthesis* **2002**, *8*, 1101–1109.
(29) Ulrich, G.; Bedel, S.; Picard, C. *Tetrahedron Lett.* **2002**, *43*, 8835–8837.
(30) Comby, S.; Imbert, D.; Chauvin, A.-S.; Bünzli, J.-C. G.; Charbonnière, L. J.; Ziessel, R. F. *Inorg. Chem.* **2004**, *43*, 7369–7379.
(31) Latva, M.; Takalo, H.; Mukkala, V. M.; Matachescu, C.; Rodriguez-Ubis, J. C.; Kankare, J. *J. Lumin.* **1997**, *75*, 149–169.
(32) (a) Bretonnière, Y.; Mazzanti, M.; Pécaut, J.; Olmstead, M. M. *J. Am. Chem. Soc.* **2002**, *124*, 9012–9013. (b) Charbonnière, L. J.; Mameri, S.; Flot, D.; Waltz, F.; Zandanel, C.; Ziessel, R. *Dalton Trans.* **2007**, 2245–2253.
(33) Tsukube, H.; Shinoda, S. *Chem. Rev.* **2002**, *102*, 2389–2404.
(34) Parker, D. *Coord. Chem. Rev.* **2000**, *205*, 109–130.
(35) (a) Bretonnière, Y.; Cann, M. J.; Parker, D.; Slater, R. *Org. Biomol. Chem.* **2004**, *2*, 1624–1632. (b) Tremblay, M. S.; Halim, M.; Sames, D. *J. Am. Chem. Soc.* **2007**, *129*, 7570–7577.
(36) (a) Song, B.; Wang, G.; Tan, M.; Yuan, J. *J. Am. Chem. Soc.* **2006**, *128*, 13442–13450. (b) Atkinson, P.; Bretonnière, Y.; Parker, D. *Chem. Commun.* **2004**, 438–439.
(37) Charbonnière, L.; Ziessel, R.; Montalti, M.; Prodi, L.; Zaccheroni, N.; Boehme, C.; Wipff, G. *J. Am. Chem. Soc.* **2002**, *124*, 7779–7788.
(38) (a) Baaden, M.; Berny, F.; Boehme, C.; Muzet, N.; Schurhammer, R.; Wipff, G. *J. Alloys Compd.* **2000**, *303–304*, 104–111. (b) Li, S.-H.; Yuan, W.-T.; Zhu, C.-Q.; Xu, J.-G. *Anal. Biochem.* **2004**, *331*, 235–242.
(39) Hirsch, A. K. H.; Fischer, F. R.; Diederich, F. *Angew. Chem., Int. Ed.* **2007**, *46*, 338–352.
(40) Charbonnière, L. J.; Schurhammer, R.; Mameri, S.; Wipff, G.; Ziessel, R. F. *Inorg. Chem.* **2005**, *44*, 7151–7160.
(41) Mameri, S.; Charbonnière, L. J.; Ziessel, R. F. *Inorg. Chem.* **2004**, *43*, 1819–1821.

Scheme 2. Synthetic Protocols for Obtaining Ligands **L1**−**L3**[a]

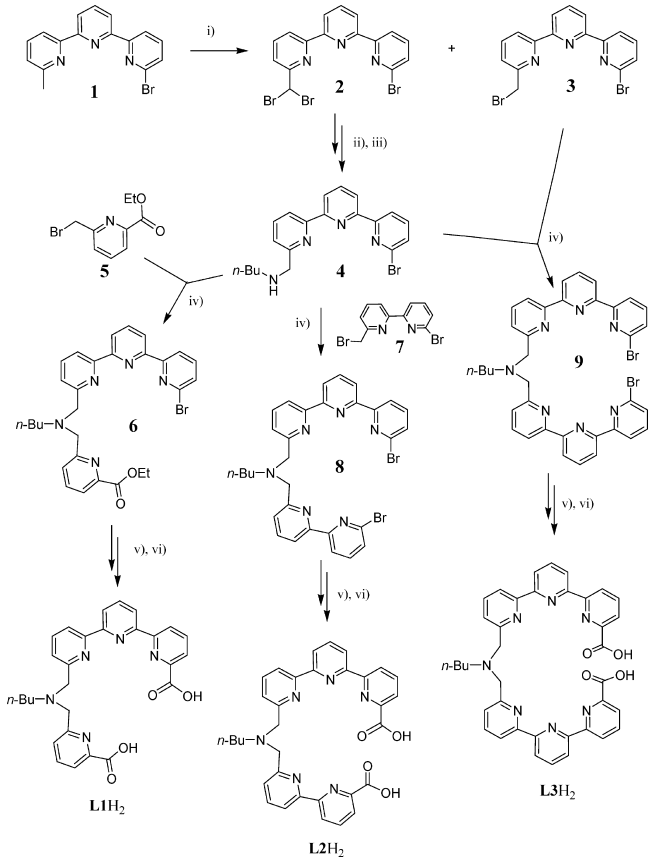

[a] Legend: (i) NBS, *hν*, AIBN, refluxing benzene, 65% for **2** (5 equiv of NBS), 65% for **3** (1 equiv of NBS);[32b] (ii) ^{n}BuNH$_2$, CH_3CN, K_2CO_3, 80 °C; (iii) $NaBH_4$, EtOH, 70 °C (quantitative for the two steps); (iv) CH_3CN, K_2CO_3, 80 °C (87% for **6**, 82% for **8**, and 87% for **9**); (v) [Pd(PPh$_3$)$_2$Cl$_2$], EtOH, Et$_3$N, CO (1 atm), 70 °C (80, 89, and 94% respectively for the intermediate esters of **L1**−**L3**); (vi) concentrated HCl, 80 °C (70, 95, and 87%, respectively, for **L1**−**L3**).

Results and Discussion

Synthesis of the Ligands and Complexes. The synthesis of the ligands is illustrated in Scheme 2. The pivotal terpyridine fragment **1** was obtained according to literature procedures.[32b] A radical bromination of **1** using NBS in refluxing benzene afforded a mixture of the monobrominated terpyridine **3** and the *gem*-dibromoterpyridine **2**. By varying the proportion of brominating agent relative to **1**, it was possible to optimize the synthesis for preparation of **3** (65% with 1.3 equiv of NBS/**1**) or of **2** (65% with 5.0 equiv of NBS/**1**). From the dibromo compound **2**, a reaction with *n*-butylamine in CH_3CN containing K_2CO_3 as a base afforded the intermediate imine,[42] which was reduced with $NaBH_4$ into the secondary amine **4** in quantitative yield. Alkylation of **4** with the pyridine precursor **5** afforded the intermediate **6** (87% yield). A carboalkoxylation reaction[43] allowed for conversion of the bromo function into an ethyl ester group in 80% yield, and the diester was subsequently hydrolyzed with concentrated HCl to afford the ligand **L1**H_2 in 70% yield as the trihydrochloride salt.

When alkylation of **4** was performed with the 6-bromo-6′-methyl-2,2′-bipyridine **7**,[44] the tertiary amine **8** was obtained, which can also be submitted to the same carboalkoxylation/hydrolysis sequence used for **6**, to generate

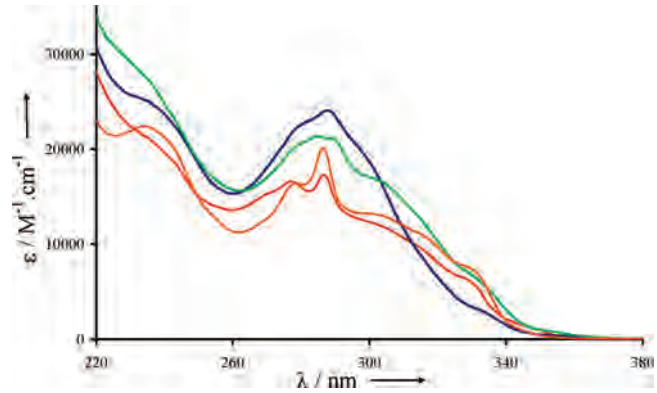

Figure 1. UV–vis absorption spectra of the ligands **L1** (red), **L2** (blue), **L3** (green), and **L4** (orange) in water (TRIS/$HClO_4$, pH 7.0, 0.01 M).

respectively the intermediate diester (89%) and **L2**H_2 (95%) as its hydrochloride salt. Similarly, alkylation of **4** with **3** afforded the bis-terpyridyl−butylamine **9**, which was converted into **L3**H_2 as its trihydrochloride salt by a similar carboalkylation/hydrolysis protocol.

The Eu and Tb complexes of ligands **L1**−**L3** were obtained by mixing equimolar amounts of the protonated ligands and of the hexahydrate chloride salts of the Ln precursors in hot MeOH/H_2O mixtures. After a few hours, the solutions were neutralized with Et_3N and concentrated under vacuum and the complexes were precipitated by addition of diethyl ether. The complexes were characterized by IR spectroscopy, elemental analysis, and FAB$^+$ mass spectrometry. For the Eu complexes of **L2** and **L3**, the mass spectrometry unambiguously confirmed a ligand to Ln ratio of 1:1, in accord with the isotopic pattern of the Eu**L**$^+$ peak, showing a difference of 2 *m*/*z* units that corresponds to Eu^{151} (48%) and Eu^{153} (52%).

Photophysical Properties of the Ligands and Complexes. The UV–vis absorption spectra of the ligands in aqueous solutions at pH 7.0 are presented in Figure 1. All spectra displayed broad absorption bands in the UV domain with maxima at 285–288 nm. These absorption bands are typical of $\pi \rightarrow \pi^*$ transitions centered on the bipyridine[45,46] or terpyridine moieties,[46a] and their high energy position points to all trans conformations between adjacent pyridyl cycles.[46a] Apart from the presence of a narrow absorption band at 287 nm in **L1**, which is typical of the terpyridine units,[46a,47] it is not possible from these spectra to differentiate the relative contributions of the various polypyridine units present in the ligands. The absorption maxima are found at 287 (ϵ = 17 200 M^{-1} cm^{-1}), 288 (ϵ = 24 100 M^{-1} cm^{-1}),

(42) Weibel, N.; Charbonnière, L. J.; Ziessel, R. F. *J. Org. Chem.* **2002**, *67*, 7876–7879.
(43) El Ghayouri, A.; Ziessel, R. *J. Org. Chem.* **2000**, *65*, 7757–7763.
(44) Mameri, S.; Charbonnière, L. J.; Ziessel, R. F. *Synthesis* **2003**, *17*, 2713–2719.
(45) Westheimer, F. H.; Benfey, O. T. *J. Am. Chem. Soc.* **1956**, *78*, 5309–5311.
(46) (a) Nakamoto, K. *J. Phys. Chem.* **1960**, *64*, 1420–1425. (b) Krumholtz, P. *J. Am. Chem. Soc.* **1951**, *73*, 3487–3492.
(47) Prodi, L.; Montalti, M.; Zaccheroni, N.; Pickaert, G.; Charbonnière, L.; Ziessel, R. *New J. Chem.* **2003**, *27*, 134–139.
(48) Haas, Y.; Stein, G. *J. Phys. Chem.* **1971**, *75*, 3668–3677.
(49) Nakamura, K. *Bull. Chem. Soc. Jpn.* **1982**, *55*, 2697–2705.
(50) Olmsted, J. *J. Phys. Chem.* **1979**, *83*, 2581–2584.

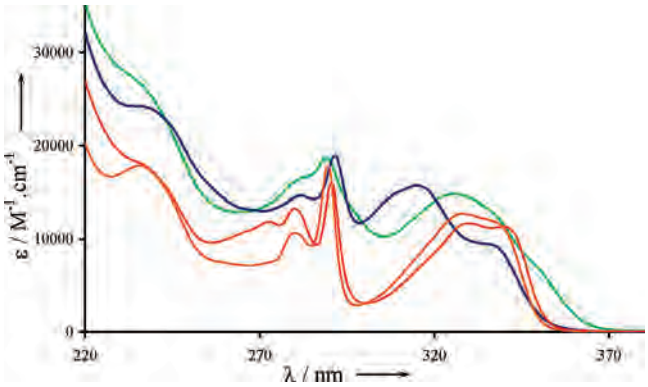

Figure 2. UV–vis absorption spectra of the Eu complexes of ligands **L1** (red), **L2** (blue), **L3** (green), and **L4** (orange) in water (TRIS/$HClO_4$, pH 7.0, 0.01 M).

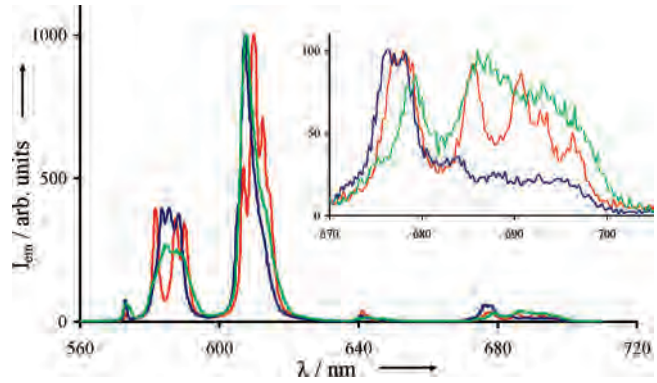

Figure 3. Emission spectra of the europium complexes of **L1**−**L3** in water (TRIS/HCl, 0.01 M, pH 7.0, cutoff filter at 390 nm, λ_{exc} = 335, 337, and 330 nm, respectively, for **L1** (red), **L2** (blue), and **L3** (green)) normalized to unity for emission from 575 to 607 nm. Inset: expansion of the $^5D_0 \rightarrow {}^7F_4$ region (normalized at the maxima in this region).

and 285 nm (ϵ = 21 400 M^{-1} cm^{-1}), respectively, for **L1**−**L3** (TRIS/$HClO_4$, pH 7.0, 0.01 M).

In contrast, the shapes of the absorption spectra of the resulting lanthanide complexes in the same solvent are particularly informative. Upon complexation, the $\pi \rightarrow \pi^*$ transitions centered on the polypyridyl moieties split into at least two components, with appearance of a large bathochromic shift. The effect is almost identical for complexation of europium or terbium, but the splitting is very different, depending on the ligand. The absorption spectra of the Eu complexes of the ligands **L1**−**L3** are displayed in Figure 2, together with the spectrum of the Eu complex of **L4**,[32b] for the purpose of comparison. The spectrum of the [Eu(**L4**)-$(H_2O)_2$]$^+$ complex in water shows the coordinated terpyridine unit to present a strong absorption band at 327 nm and the presence of a fine structure at 340 nm, a signature of the coordinated terpyridine unit observed, for example, in the [Zn(terpy)Cl]Cl complex.[46a] Similarly, the europium complex of **L1** displays the same absorption band slightly red-shifted and a very similar overall absorption spectrum, except for a stronger absorption around 275 nm, associated with the pyridyl carboxylate arm.[18,19] Unfortunately, the electronic changes brought about by the complexation of such strands did not lead to strong spectroscopic changes, as observed with bipy[28,30] or terpy[47] chelating systems, and although it is highly probable, it can not be unambiguously confirmed that the pyridyl arm is coordinated to the Eu cation. Interestingly, the fine structure of the low-energy absorption band is more marked than in the **L4** complex, suggesting a decrease in vibrational motions possibly attributed to a strengthened complexation. The spectrum of the Eu complex of **L2** displays an intense additional band at 315 nm, clearly associated with the coordination of the bipyridyl arm in a cis conformation,[28,30] together with the contribution of the coordinated terpyridyl unit appearing as a shoulder at lower energy (340 nm). Finally, the case of the Eu complex of **L3** appears to be more complicated, as the low-energy absorption band is broadened, with the presence of an ill-defined absorption band around 285 nm, as observed in the free ligand (Figure 1). It is worth noting that the absorption around 305 nm is more pronounced than in the complexes of **L1** and **L4** and that there is a large absorption appearing in the 350–370 nm region. The observation of these changes is in perfect agreement with the spectral signature of the terpyridine moiety, as observed at intermediate pH in its monoprotonated form.[46a] In that case, the conformation of the terpyridine core was attributed to a cis,trans conformation of the adjacent pyridyl rings. The observed spectra suggest a mixture of two conformations for the terpyridyl arms (one cis,cis and one cis,trans) and likely the coordination of only one of the two terpyridyl arms, the second being in an intermediate configuration.

Further insights into the spectroscopic characterization of the complexes in water solution were obtained by luminescence spectroscopy. Upon excitation into the absorption bands of the UV–vis domain, all of the complexes display the typical narrow emission bands of the europium or terbium cations. The emission spectra of the Eu complexes of **L1**−**L3** are displayed in Figure 3, while those of Tb are presented in Figure MS1 (Supporting Information). Interestingly, no residual fluorescence of the ligand could be observed, whatever the complex studied. For the Eu complexes (Figure 3), the expected $^5D_0 \rightarrow {}^7F_J$ (J = 0−4) transitions of Eu are observed,[51] $^5D_0 \rightarrow {}^7F_0$ being clearly observed in the 570–575 nm region. If the overall shapes of the spectra are very similar, the $^5D_0 \rightarrow {}^7F_4$ transitions ranging from 675 to 705 nm are very sensitive to the environment,[51] and are different in shape for all complexes, pointing to different coordination environments around the Eu cation (inset in Figure 3). Also very informative, the region of the $^5D_0 \rightarrow {}^7F_1$ transitions from 575 to 600 nm clearly displays three components for the complexes of **L1** and **L2**, pointing to a low symmetry.[51] In contrast, the corresponding spectrum for the complex of **L3** only showed a broad unstructured band, which may be correlated to fluxional motions in the complex, as confirmed by NMR studies in solution (vide infra).

The excitation spectra recorded upon metal-centered emission are all very similar to the corresponding absorption spectra (Figure MS2 (Supporting Information)). Thus, even if some polypyridine arms are not fully coordinated to the lanthanide cations, as suspected for **L3** for example, the

(51) Bünzli, J.-C. G. In *Lanthanide Probes in Life, Chemical and Earth Sciences: Theory and Practice*; Bünzli, J.-C. G., Choppin, G. R., Eds.; Elsevier: Amsterdam, 1989.

Table 1. Photophysical Properties of the Eu and Tb Complexes of Ligands **L1**−**L3** in Aqueous Solution (TRIS/$HClO_4$, pH 7.0, 0.01 M)

			emission		
ligand	Ln	abs λ/nm (ϵ/M^{-1} cm^{-1})	ϕ_{H_2O}[a]	τ_{H_2O} (τ_{D_2O})/μs	q[b]
L1	Eu	280 (13 800), 290 (15 700), 330 (11 500), 340 (11 200)	5.7	390 (2060)	2.0 (2.2)
	Tb	280 (13 900), 290 (15 800), 330 (11 700), 340 (11 300)	32	850 (1400)	1.9 (2.0)
L2	Eu	291 (18 800), 315 (16 000), 335 (9800)	3.7	410 (2180)	1.9 (2.1)
	Tb	291 (19 000), 315 (16 100), 335 (10 000)	6.1	590 (810)	1.9 (2.0)
L3	Eu	289 (18 700), 326 (15 800)	0.5	360 (2060)	2.2 (2.4)
	Tb	289 (18 900), 326 (16 100)	1.2	460 (600)	2.1 (2.2)
L4[32b]	Eu	290 (17 600), 328 (12 000)	6.5	420 (2290)	1.8 (2.0)
	Tb	290 (17 900), 328 (12 300)	22	920 (1600)	1.9 (2.0)

[a] Determined according to ref 48 using $[Ru(bipy)_3]Cl_2$ in nondegassed water ($\phi = 2.8\%$[49]) for europium and both Rhodamine 6G in ethanol ($\phi = 88\%$[50]) and the terbium complex of ref 28a in water ($\phi = 31\%$). [b] Determined according to ref 14a for Eu, ref 14b for Tb, and ref 14c for Eu and Tb (values in parentheses).

uncoordinated arms give rise to efficient energy transfer to the cations.

The overall luminescence quantum yields of the complexes were determined in buffered water solutions (Table 1). For both series of complexes, the quantum yield decreases with an increasing number of pyridine rings. In the case of **L1**, the quantum yield is very large, improving the data previously observed for **L4**,[32b] in good agreement with complexes based on genuine terpyridine.[31] In contrast, for both Tb and Eu, the quantum yields sharply drop for ligand **L2** and even more with **L3**. A very surprising result arose from the measurements of luminescence lifetimes of the complexes in water and deuterated water. For the same solvent, the lifetimes are almost identical for the whole series of Eu complexes. The calculation of the number of water molecules coordinated in the first sphere of the cations indicated the presence of two inner-sphere water molecules for all complexes. According to these results and in agreement with the results of elemental analysis and mass spectrometry, a generic formula of $[LnL\boldsymbol{X}(H_2O)_2]^+$ can be suggested.

^{1}H NMR Study of the Europium Complexes. A first set of data concerning the coordination behavior in solution was obtained using ^{1}H NMR spectroscopy in D_2O. As shown in Figure 4, the spectrum of $[Eu(\mathbf{L1})(H_2O)_2]Cl$ displayed 17 distinct peaks integrating for the 25 expected protons.

As expected, the spectrum is spread over 22 ppm, as a result of the paramagnetic contribution of the europium atom.[1] Interestingly, almost all peaks display a clear hyperfine structure, despite the expected enlargement due to this paramagnetic contribution. In contrast, the spectrum of $[Eu(\mathbf{L2})(H_2O)_2]Cl$ is less expanded over the spectral window, covering only 14 ppm (Figure 4, bottom). Here the peaks are broad and poorly defined and most of the hyperfine structures are lost. Finally, the spectrum of $[Eu(\mathbf{L3})(H_2O)_2]Cl$ only displayed very broad peaks (not shown). These results point to the possibility of a weakening of the coordination strength of the ligands from **L1** to **L3**. The complex formed with **L1** appeared clearly defined as a result of a strong coordination. Molecular motions of the ligand around the Eu center are minimized, and this translates to well-resolved signals with hyperfine structures, and the proximity of the paramagnetic center is correlated to a larger spectral expansion. Increasing the number of pyridine rings in the ligands resulted in a weakening of the coordination, probably as a result of prononced steric constraints. This weakening is

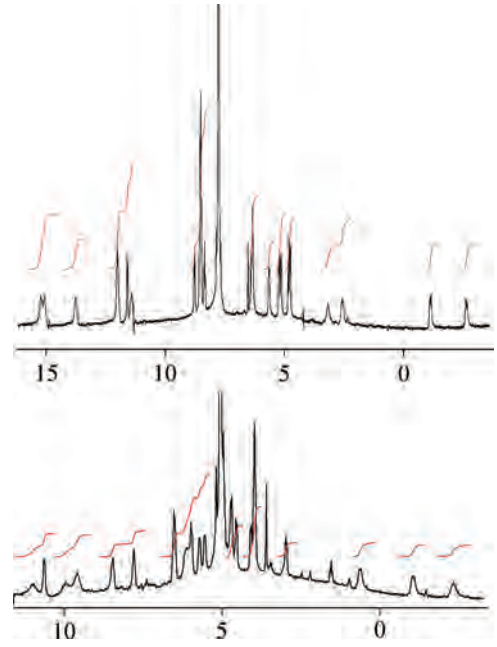

Figure 4. ^{1}H NMR spectra of $[Eu(\mathbf{L1})(H_2O)_2]Cl$ (top) and $[Eu(\mathbf{L2})(H_2O)_2]Cl$ (bottom) in D_2O (200 MHz).

observed in a progressive enlargement of the peaks consecutive to larger vibrational motions of the ligands relative to the Eu center. It may also be linked to the narrower spectral window observed for the complex of **L2**, assuming that the weakest coordination is related to a remoteness of the H−Eu distances that can be directly related to a decrease of the dipolar contribution to the paramagnetic shift.[1] Finally, these results are in good agreement with the observed decrease of the luminescence quantum yields along the series **L1**−**L3**. Increasing the number of pyridine rings leads to a destabilization of the coordination with increased vibrational deactivation processes for the lanthanide excited state together with a decrease of the efficiency of the ligand to metal energy transfer process due to remoteness of the ligands.

DFT Calculations. Despite all our efforts, we have been unable to crystallize the complexes with sufficient quality for X-ray diffraction analysis. In order to obtain structural information on the complexes presented in this work, the $[Eu(\mathbf{L1'})(H_2O)_2]^+$, $[Eu(\mathbf{L2'})(H_2O)_2]^+$, and $[Eu(\mathbf{L3'})(H_2O)_2]^+$ systems were then investigated by means of density functional theory (DFT) calculations at the B3LYP/6-31G(d)

Table 2. Bond Distances (Å) of the Metal Coordination Environment Obtained from DFT Calculations[a]

	$[Eu(\mathbf{L1'})(H_2O)_2]^+$		$[Eu(\mathbf{L2'})(H_2O)_2]^+$		$[Eu(\mathbf{L3'})(H_2O)_2]^+$	
	in vacuo	in soln	in vacuo	in soln	in vacuo	in soln
Eu−N1	2.858	2.812	2.910	2.870	4.291	4.244
Eu−N2	2.727	2.661	2.829	2.713	2.844	2.793
Eu−N3	2.728	2.668	3.075	2.789	2.613	2.610
Eu−N4	2.633	2.590	2.723	2.631	2.540	2.553
Eu−N5	2.557	2.585	2.761	2.867	4.680	4.753
Eu−N6			2.631	2.783	3.979	4.162
Eu−N7					2.828	3.031
Eu−O1	2.351	2.416	2.316	2.416	2.309	2.335
Eu−O2	2.701	2.545	2.626	2.596	2.580	2.497
Eu−O3	2.722	2.549	2.809	2.617	2.494	2.450
Eu−O4	2.257	2.377	2.301	2.423	2.258	2.295

[a] See Figure 5 for labeling scheme.

level. For computational simplicity in these calculations the butyl groups of ligands **L1**−**L3** were substituted by methyl groups, the methyl-substituted ligands being denoted as **L1′**−**L3′**, respectively. The in vacuo optimized geometries of the $[Eu(\mathbf{L1'})(H_2O)_2]^+$ and $[Eu(\mathbf{L2'})(H_2O)_2]^+$ systems show relatively long Eu−O_W distances (O_W = oxygen atom of inner-sphere water molecules; Table 2), as often observed when Ln complexes are studied in vacuo by means of quantum mechanical calculations.[52] Thus, we turned to geometry optimizations including the surrounding solvent effects (water) by using the polarized continuum model (PCM). The B3LYP/PCM approach has been successfully used to describe the structure in aqueous solution of Ln(III) aquo ions and other lanthanide complexes.[53] The Eu−O_W distances calculated in aqueous solution are substantially shorter than those calculated in vacuo. The shortening of the Eu−O_W bond distances observed in solution can be ascribed to a stronger water-ion interaction due to the solvent polarization effects that, increasing the dipole moment of the free water molecules, increase the water-ion interaction. The distances calculated in aqueous solution fall in the normal range observed in the solid state for different europium complexes.[54] This is in agreement with the luminescence lifetime measurements described above, which indicated the presence of two inner-sphere water molecules in this family of complexes. The in vacuo optimized structures exhibit bond lengths Ln−N_{AM} and Ln−N_{PY} (N_{AM} = amine nitrogen atom, N_{PY} = pyridyl nitrogen atom) that are longer than those usually observed for Eu complexes with polyamino carboxylate ligands, while the Ln−O_C bonds are close to the experimental values. In solution, Ln−N bond lengths are shorter, whereas Ln−O_C bond lengths are slightly increased, providing a generally better agreement with typical experimental bond lengths obtained for polyamino carboxylate chelates. Thus, in the following we will focus our attention on the structures of the complexes optimized in aqueous solution.

The structure of $[Eu(\mathbf{L1'})(H_2O)_2]^+$ optimized in aqueous solution (Figure 5) indicated an almost planar coordination of the terpyridinecarboxylate unit, with the podand nitrogen atom being slightly displaced down the average coordination plane. A similar conformation of the ligand has been observed in the solid state for the dimer $[Gd_2(\mathbf{L4})_2(H_2O)_2]$.[32b] The coordination of the pyridinecarboxylate arm occurred over the plane of the terpyridinecarboxylate unit, while the two inner-sphere water molecules are placed below that plane. This leads to an overall coordination number of 9 for the complex, due to the coordination of the heptadentate ligand and the two water molecules. The introduction of a second pyridine ring in **L2′** leads to a complex having both bipy and terpy strands fully coordinated to the Ln atom, in agreement with the UV–vis absorption spectra (see above). However, the lengthening of the second arm brings some steric repulsions within the coordinated terpyridinecarboxylate arm. As a result, the terpyridinecarboxylate arm did not adopt a planar conformation, the N(3)−C−C−N(4) dihedral angle being ca. 18° (ca. 4° in the complex of **L1′**). In $[Eu(\mathbf{L2'})(H_2O)_2]^+$ two coordination sites remained accessible for water molecules at the lower part of the coordination sphere (Figure 5), in agreement with luminescence lifetime data. As a result, the overall coordination number of the complex increased from 9 to 10 upon introduction of an additional pyridine unit in the ligand framework. It must be pointed out that even if the most commonly observed coordination numbers in Ln complexes are 8 and 9, several examples of 10-coordinated lanthanide complexes have been reported in the literature.[19,55] The structure of $[Eu(\mathbf{L2'})(H_2O)_2]^+$ calculated in aqueous solution presented distances between the metal ion and the nitrogen atoms of the terpy unit ranging from 2.63 to 2.79 Å. These distances are substantially shorter than the Eu−N5 distance, where N5 is one of the nitrogen atoms of the bipy fragment (Figure 5). These results suggest that the strongest coordination to the lanthanide is provided by the terpyridinecarboxylate group rather than by the bipyridinecarboxylate arm.

Finally, the introduction of the third pyridyl ring on the second coordinating arm results in large changes in the Eu coordination environment. The structure of $[Eu(\mathbf{L3'})(H_2O)_2]^+$ optimized in aqueous solution (Figure 5) shows the Eu ion being only 7-coordinated by the three nitrogen atoms and the carboxylate group of one of the terpyridinecarboxylate arms and the carboxylate group of the second terpyridinecarboxylate unit, 7-coordination being completed by the presence of two inner-sphere water molecules. The pivotal nitrogen atom and the three nitrogen atoms of one of the terpyridine carboxylate arms either remain uncoordinated or show a weak interaction with the metal ion (Eu−N = 3.03–4.75 Å). The coordinated terpy unit adopts a relatively

(52) (a) Platas-Iglesias, C.; Mato-Iglesias, M.; Djanashvili, K.; Muller, R. N.; Vander Elst, L.; Peters, J. A.; de Blas, A.; Rodríguez-Blas, T. *Chem. Eur. J.* **2004**, *10*, 3579–3590. (b) Cosentino, U.; Villa, A.; Pitea, D.; Moro, G.; Barone, V.; Maiocchi, A. *J. Am. Chem. Soc.* **2002**, *124*, 4901–4909.

(53) (a) Djanashvili, K.; Platas-Iglesias, C.; Peters, J. A. *Dalton Trans.* **2008**, 602–607. (b) Georgieva, I.; Trendafilova, N.; Aquino, A. J. A.; Lischka, H. *Inorg. Chem.* **2007**, *46*, 10926–10936.

(54) Alexander, V. *Chem. Rev.* **1995**, *95*, 273–342.

(55) (a) Platas, C.; Avecilla, F.; de Blas, A.; Rodríguez-Blas, T.; Bastida, R.; Macías, A.; Rodríguez, A.; Adams, H. *Dalton Trans.* **2001**, 1699–1705. (b) Valencia, L.; Martínez, J.; Macías, A.; Bastida, R.; Carvalho, R. A.; Geraldes, C. F. G. C. *Inorg. Chem.* **2002**, *41*, 5300–5312. (c) Bligh, S. W. A.; Choi, N.; Geraldes, C. F. G. C.; Knoke, S.; McPartlin, M.; Sanganee, M. J.; Woodroffe, T. M. *J. Chem. Soc., Dalton Trans.* **1997**, 4119–4126. (d) Fernandez-Fernandez, M. d. C.; Bastida, R.; Macias, A.; Perez-Lourido, P.; Platas-Iglesias, C.; Valencia, L. *Inorg. Chem.* **2006**, *45*, 4484–4496.

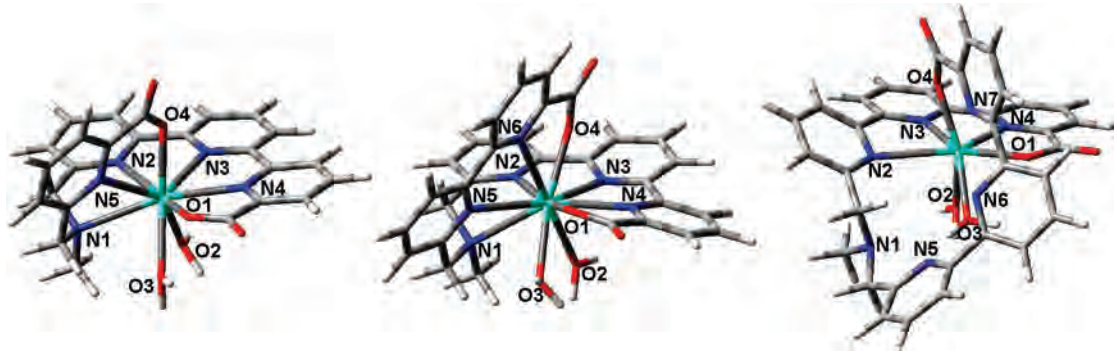

Figure 5. Calculated structures (B3LYP) of complexes $[Eu(\mathbf{L1'})(H_2O)_2]^+$, $[Eu(\mathbf{L2'})(H_2O)_2]^+$, and $[Eu(\mathbf{L3'})(H_2O)_2]^+$ in aqueous solution.

planar conformation, while the second terpy unit is far from planarity, in agreement with the UV–vis spectra of the Eu and Tb complexes described above. One of the inner-sphere water molecules is involved in a hydrogen-bonding interaction with a nitrogen atom of the uncoordinated terpy unit (O3−N5 = 2.736 Å; N5−H = 1.734 Å; O3−H−N5 = 170.9°). The relatively low coordination number observed in the calculated structure of $[Eu(\mathbf{L3'})(H_2O)_2]^+$ is attributed to the steric crowding around the Eu ion generated by the presence of the second terpyridinecarboxylate arm.

Interactions with Phosphorylated Anions. In order to scrutinize the potential of these lanthanide complexes as luminescent sensors for anion recognition, we performed a series of titration experiments following the absorption and emission changes in the presence of phosphorylated anions such as AMP^{2-}, ADP^{3-}, ATP^{4-}, and HPO_4^{2-}. The titrations were performed in water solutions containing 0.01 M of TRIS, buffered at pH 7.0. As the counterion of the acid used to buffer the solution at this pH may provide particular interactions with the charged complexes, both HCl and $HClO_4$ were used, showing no differences between the results for the different titrations. A titration experiment consisted of adding increasing amounts of the anion of interest to a solution of the europium complexes of **L1**−**L4**. After each addition, the UV–vis absorption and steady-state emission spectra of the solution were measured and, at some points of the titrations, the luminescence lifetimes at the maxima of the europium emission (610−615 nm) were also monitored and analyzed to check the possible presence of several emitting species.

The first series of titrations with $[Eu(\mathbf{L1})]^+$ and the four anions revealed a total absence of significant interactions of this complex within the series. UV–vis titrations with the adenosine anions only showed the emergence of a strong absorption band centered at 258 nm attributed to the absorption band of the aromatic adenosine moiety (Figure MS3). With the phosphate anions, no changes were observed (Figure MS4). Similarly, the luminescence intensities of the europium emission remained constant, as did the europium lifetime, with a monoexponential decay of 392 ± 8 μs.

Titrations of $[Eu(\mathbf{L2})]^+$ with AMP^{2-}, ADP^{3-}, and HPO_4^{2-} did not reveal any significant effects of the anions on the photophysical properties of the complex (Figure MS5). In contrast, the addition of ATP^{4-} resulted in clear spectral changes. Figure 6 displays the evolution of the UV–vis absorption spectra of the solution of $[Eu\mathbf{L2}]^+$ upon progressive ATP addition.

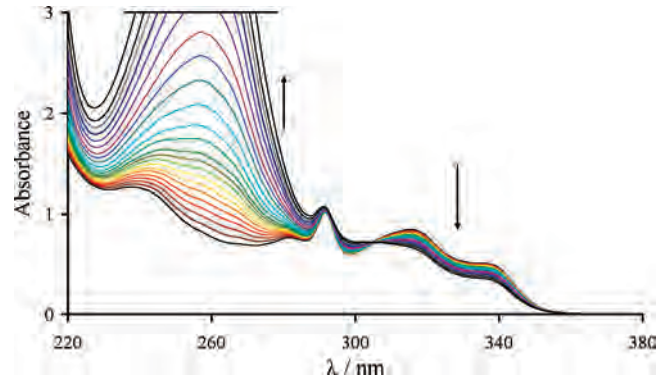

Figure 6. Evolution of the UV–vis absorption spectra of a 5.2×10^{-5} M solution of $[Eu(\mathbf{L2})]^+$ in water upon addition of increasing amounts of ATP^{4-} (0−6.3 equiv, TRIS/$HClO_4$, 0.01 M, pH 7.0, corrected for dilution).

Upon addition of ATP, the $\pi \rightarrow \pi^*$ absorption band of the bipyridyl moiety, initially occuring at 315 nm in the complex, is hypsochromically shifted, while the position of the $\pi \rightarrow \pi^*$ absorption band of the terpyridyl arm at ca. 335 nm remains unchanged. This observation suggests the decoordination of the bipyridyl arm, in agreement with the weaker coordination of the bipy fragment in comparison to the terpy one suggested by DFT calculations (see above). Monitoring the changes in emission spectra revealed a gradual decrease of the emission intensity of the europium-centered bands (Figure 7), with a concomitant increase of the emission band at ca. 400 nm, attributed to the fluorescence of the decoordinated bipy arm.

Surprisingly, the observed luminescence lifetime of the complex apparently remained constant, but a careful deconvolution of the intensity decay at high ATP concentrations (Figure 8) revealed the presence of a second emitting species with a very short lifetime of 77 ± 10 μs amounting to 9% (details on the fitting procedures and calculations of the relative amounts can be found in the Supporting Information). As it was previously shown that europium sensitization by adenosine is inefficient,[41] this new species is temptatively assigned to the formation of a ternary species containing one ligand, one europium atom, and an ATP molecule ligated in the first coordination sphere.

With regard to the $[Eu(\mathbf{L3})]^+$ complex, the titration experiments revealed that AMP^{2-} displayed no interaction

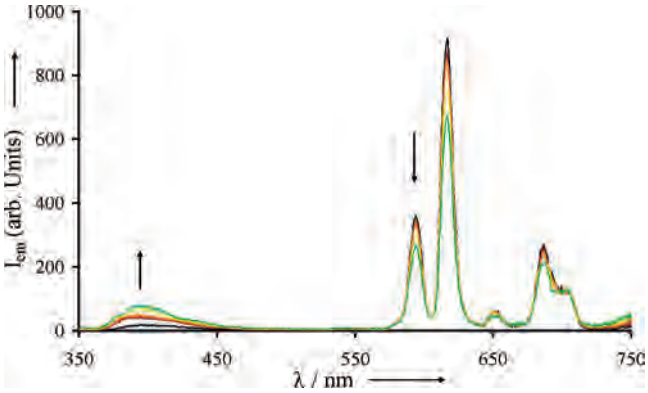

Figure 7. Evolution of the emission spectra of a 5.2×10^{-5} M solution of $[Eu(\mathbf{L2})]^{+}$ upon addition of 0, 1, 2, 3, 6, and 10 equiv of ATP^{4-} (λ_{exc} = 337 nm, cutoff filter at 390 nm).

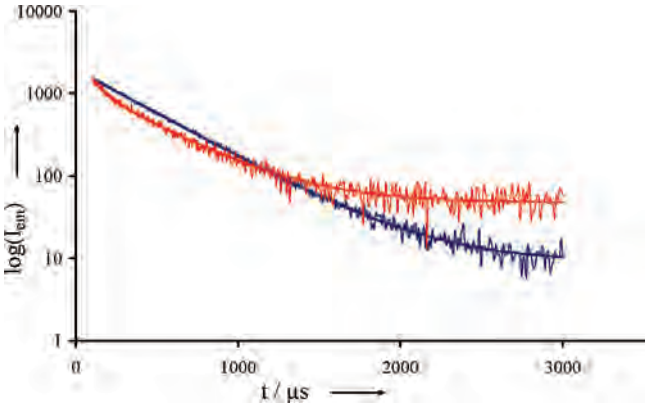

Figure 8. Normalized intensity decay (λ_{exc} = 290 nm, λ_{em} = 615 nm) of the europium emission in $[Eu(\mathbf{L2})]^{+}$ in the presence of 0 (blue) and 8 equiv of ATP^{4-} (red) and the corresponding mono- and biexponential fitting decay function (see text).

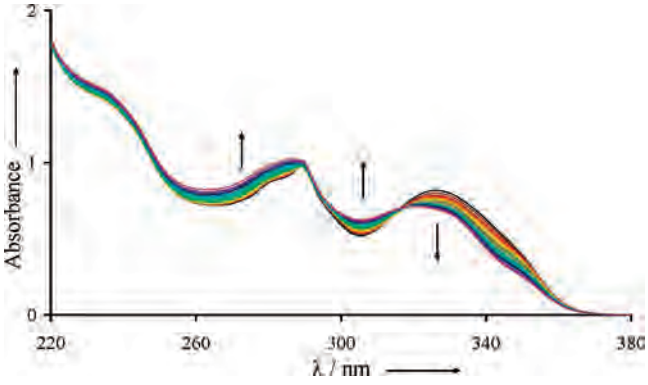

Figure 9. Evolution of the UV–vis absorption spectra of a solution 5.1×10^{-5} M in $[Eu(\mathbf{L3})]^{+}$ upon addition of increasing amounts of HPO_4^{2-} anions (0−6 equiv).

with the complex, whereas ADP^{3-}, ATP^{4-}, and HPO_4^{2-} all have interactions and showed impact on the absorption, emission, and luminescence lifetimes. Figure 9 illustrates the observed absorption changes for titration with HPO_4^{2-}, while the corresponding absorption and emission experiments for the other anions are gathered in Figures MS7−MS11. The case of HPO_4^{2-} is very informative, showing the $\pi \rightarrow \pi^*$ transition of the terpyridyl moieties to be moderately displaced toward higher energies, probably as a result of the decoordination of one of the terpy arms. The presence of an isosbestic point at 316 nm suggests the presence of only two absorbing species, one of which is the precursor complex.

Scheme 3. Fragments of Ligand **L2** Used To Model the Interaction of $[Eu(\mathbf{L2})]^{+}$ with ATP^{4-}

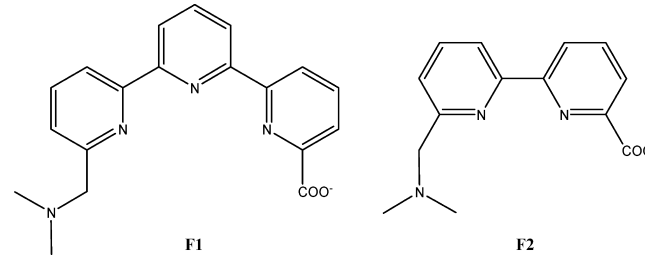

Interestingly, in all cases where interaction took place, one can observe that the average luminescence lifetime for europium emission at 615 nm increased. Applying a biexponential fitting procedure always greatly improved the results (according to the Durbin−Watson fitting parameter), indicating the coexistence of two emitting species: the precursor complex and a new complex assigned as the ternary adduct. In parallel, where interaction with the anion took place, the emission spectra of the solution revealed the increase of the ligand fluorescence around 400 nm (Figures MS7−MS9), probably arising from the partial decoordination of one terpy strand. The DFT calculations described above support this hypothesis, as they show a weak binding of one of the terpyridinecarboxylate units to the Eu ion.

All these results point to the formation of ternary species containing the europium atom, the **L3** ligand, and an anion, as previously observed for the interaction of $[Eu(\mathbf{L2})]^{+}$ with ATP^{4-}. Unfortunately, while the observed changes are clearly indicative of the formation of a ternary species, they could not be treated quantitatively, as a result of the weakness of the observed spectroscopic changes. Only in the best case of interaction of ATP^{4-} with $[Eu(\mathbf{L3})]^{+}$ could we estimate an upper limit of the association constant leading to the formation of the ternary adduct of 1.5×10^{3} M^{-1}.

DFT Studies on the Interaction of $[Eu(L2)]^{+}$ with ATP^{4-}. To obtain insights into the structural consequences of the interaction of $[Eu(\mathbf{L2})]^{+}$ with ATP^{4-}, the tertiary complexes formed by Eu, **L2′**, and MeTP were characterized by means of DFT calculations at the B3LYP/6-31G(d) level. In these calculations ATP^{4-} was mimicked by its simplified methyl analogue, assuming that it binds similarly to the complex.[40] The following strategy was used. In the first step, the tertiary complexes formed between MeTP, Eu, and fragments **F1** and **F2** shown in Scheme 3 were investigated. Since the formation of the tertiary complex results from the competitive interactions of the ligand, the anion, and the solvent, two water molecules were initially included in the model. However, geometry optimizations carried out on the $[Eu(\mathbf{F1})(MeTP)(H_2O)_2]^{2-}$ system showed that neither of the two water molecules included in the model remained coordinated to the metal ion and that only one of the water molecules remained coordinated for $[Eu(\mathbf{F2})(MeTP)(H_2O)_2]^{2-}$. Taking these results into account, full geometry optimizations were carried out on the $[Eu(\mathbf{F1})(MeTP)]^{2-}$ and $[Eu(\mathbf{F2})(MeTP)(H_2O)]^{2-}$ systems. Once convergence was

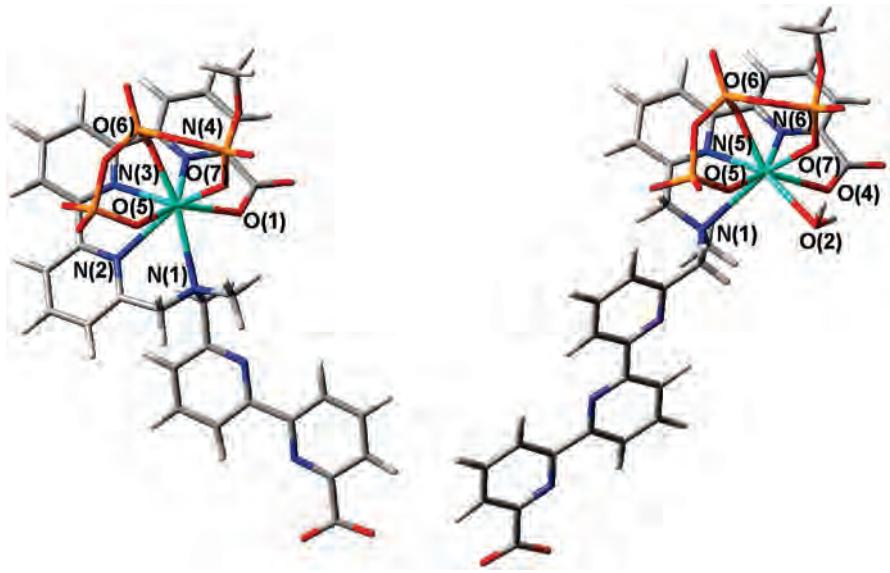

Figure 10. Calculated structures (B3LYP/6-31G(d)) of the $[Eu(\mathbf{L2'})(MeTP)]^{3-}$ (left) and $[Eu(\mathbf{L2'})(MeTP)(H_2O)]^{3-}$ systems (right).

Table 3. Bond Distances (Å) of the Metal Coordination Environment Obtained from DFT Calculations for the $[Eu(\mathbf{L2'})(MeTP)]^{3-}$ and $[Eu(\mathbf{L2'})(MeTP)(H_2O)]^{3-}$ Systems[a]

	$[Eu(\mathbf{L2'})(MeTP)]^{3-}$	$[Eu(\mathbf{L2'})(MeTP)(H_2O)]^{3-}$
Eu−N1	2.861	2.998
Eu−N2	2.771	
Eu−N3	2.815	
Eu−N4	2.687	
Eu−N5		2.776
Eu−N6		2.713
Eu−O1	2.509	
Eu−O2		2.621
Eu−O4		2.585
Eu−O5	2.273	2.204
Eu−O6	2.297	2.284
Eu−O7	2.309	2.346

[a] See Figure 10 for labeling scheme.

achieved, the second step consisted of including the fragments of **L2′** missing in **F1** and **F2**. Subsequent geometry optimizations gave the calculated structures for the $[Eu(\mathbf{L2'})(MeTP)]^{3-}$ and $[Eu(\mathbf{L2'})(MeTP)(H_2O)]^{3-}$ systems shown in Figure 10. Calculated bond lengths of the metal coordination environment for both tertiary complexes are given in Table 3.

The relative stability in aqueous solution of the $[Eu(\mathbf{L2'})(MeTP)]^{3-}$ species with respect to the $[Eu(\mathbf{L2'})(MeTP)(H_2O)]^{3-}$ one was determined by calculating the free energy variation (ΔG_{react}) for the reaction

$$[Eu(\mathbf{L2'})(MeTP)]^{3-}(sol) + H_2O(sol) \rightarrow [Eu(\mathbf{L2'})(MeTP)H_2O]^{3-}(sol)$$

We obtained $\Delta G_{react} = 54.9$ kcal mol^{-1} (328 kJ mol^{-1}), which indicates that the $[Eu(\mathbf{L2'})(MeTP)]^{3-}$ species is the most stable one in aqueous solution. These results suggest that the interaction of the $[Eu(\mathbf{L2})]^{+}$ complex with ATP^{4-} results in the decoordination of the bipyridyl arm, in agreement with the experimental evidence provided by the UV–vis absorption spectra (see above).

The optimized structure of the $[Eu(\mathbf{L2'})(MeTP)]^{3-}$ system (Figure 10) shows that the terpy unit is coordinated to the metal ion with Eu−N distances of 2.69–2.82 Å, while the distance between the metal ion and the aliphatic amine nitrogen atom, N(1), is considerably larger (2.86 Å). The bipy unit remains uncoordinated and adopts a trans conformation to reduce electron repulsion of the nitrogen lone pairs.[37] The coordination of the anion provokes an important lengthening of the Eu−O(1) bond distance ($\Delta d = 0.1$ Å, O(1) is the oxygen atom of the coordinated carboxylate group; Tables 2 and 3). The coordination of the $MeTP^{4-}$ results in a significant electron transfer to the metal ion, as indicated by the Mulliken charges calculated for the $[Eu(\mathbf{L2'})(MeTP)]^{3-}$ and $[Eu(\mathbf{L2'})(H_2O)_2]^{+}$ systems: 1.00 and 1.23 e, respectively. Coordination number 8 is completed by the coordination of the anion through the three phosphate groups in a 1 + 1 + 1 fashion (Eu−O = 2.27–2.31 Å).[40] As a consequence of anion coordination, the metal ion is placed above the plane defined by the terpy unit, the distance of europium to the mean square plane defined by N(2), N(3), N(4), and O(1) amounting to 1.38 Å.

Conclusion

Due to their biological relevance, phosphates and phosphorylated species are important analytes to be detected.[56] While numerous artificial sensors are based on purely organic receptors, metal complexes based on Zn,[57] Cu,[58] Mg,[59] Cd,[60]

(56) Aoki, S.; Kimura, E. *Rev. Mol. Biotech.* **2002**, *90*, 129–155.
(57) (a) Su Han, M.; Kim, D. H. *Angew. Chem., Int. Ed.* **2002**, *41*, 3809–3811. (b) Hoon Lee, D.; Hyun Im, J.; Uk Son, S.; Keun Chung, Y.; Hong, J.-I. *J. Am. Chem. Soc.* **2003**, *125*, 7752–7753. (c) Ojida, A.; Mito-Oka, Y.; Sada, K.; Hamachi, I. *J. Am. Chem. Soc.* **2004**, *126*, 2454–2463. (d) Hoon Lee, D.; Young Kim, S.; Hong, J.-I. *Angew. Chem., Int. Ed.* **2004**, *43*, 4777–4780. (e) Ojida, A.; Nonanka, H.; Miyahara, Y.; Tamaru, S.-I.; Sada, K.; Hamachi, I. *Angew. Chem., Int. Ed.* **2006**, *45*, 5518–5521.
(58) (a) Tobey, S. L.; Jones, B. D.; Anslyn, E. V. *J. Am. Chem. Soc.* **2003**, *125*, 4026–4027. (b) Padilla-Tosta, M. E.; Manuel Lloris, J.; Martinez-Manez, R.; Pardo, T.; Sancenon, F.; Soto, J.; Marcos, M. D. *Eur. J. Inorg. Chem.* **2001**, 1221–1226.
(59) Chen, C.-A.; Yeh, R.-H.; Lawrence, D. S. *J. Am. Chem. Soc.* **2002**, *124*, 3840–3841.
(60) Mizukami, S.; Nagano, T.; Urano, Y.; Odani, A.; Kikuchi, K. *J. Am. Chem. Soc.* **2002**, *124*, 3920–3925.

and $Fe(Cp)_2$[61] have emerged as efficient sensors. Regarding the proposed analogy between coordination chemistry of anions and that of transition metals,[62] it clearly appears that the triply charged lanthanide cations are potentially good candidates for providing sensing activity and, in fact, numerous examples can be found in the literature.[34,63] Our first approach in the field was to envisage coordination complexes containing two identical coordinating units,[40,41] such as in **L3** or, recently, two different units such as for **L1, L2**, and **L4**. The systematic increase of the number of pyridyl rings resulted in drastic changes in the coordination abilities of the ligands. The single pyridylcarboxylate arm of **L1** is perfectly suited for completing the upper part of the coordination sphere of the complexes, resulting in very stable complexes. Added anions are unable to compete with the decoordination of one arm, and the formation of ternary adducts is not observed. At the opposite, a strand composed of a terpyridylcarboxylate is too large and bulky to accommodate its full coordination to the metal ion. This weak coordination is favorable for a significant interaction with incoming anions such as ADP^{3-}, ATP^{4-}, and HPO_4^{2-}. $[Eu(\mathbf{L3})(X)]^{n-}$ ternary species are evidenced by spectrophotometric titrations. As an intermediate case, the complexes obtained with the bipyridylcarboxylate strand of **L2** showed the bipyridyl strand to be complexed in a cis conformation with coordination of the carboxylate function, as evidenced by absorption spectroscopy and confirmed by DFT calculations. Only the highly charged ATP^{4-} is able to compete with the coordination of the bipy strand, resulting in a ternary complex.

The systematic comparison of the complexes of **L1**−**L3** afforded deep insights into the understanding of the coordination of the complexes and their interactions with anions, leading to the selective interaction with ATP. Current efforts are now being directed toward the introduction of a strong coordination arm devoid of antenna effect that would allow the observation of an on–off response upon coordination of biological anions.

Experimental Section

Materials and Methods. Column chromatography and flash column chromatography were performed on silica (0.063–0.200 mm, Merck), silica gel (40–63 μm, Merck) or standardized aluminum oxide (Merck, Activity II−III). Acetonitrile was filtered over aluminum oxide and distilled over P_2O_5, DMF was distilled under reduced pressure, and diisopropylethylamine was refluxed over KOH and distilled prior to use. Other solvents were used as purchased. ^1H and ^{13}C NMR spectra were recorded on Bruker AC 200, Avance 300, and Avance 400 spectrometers operating at 200, 300, and 400 MHz, respectively, for ^1H. Chemical shifts are given in ppm, relative to residual protiated solvent.[64] IR spectra were recorded on a Nicolet 210 spectrometer as KBr pellets. Compounds **1**,[32b] **3**,[32b] and **7**[44] were obtained according to literature procedures.

Absorption and Emission Spectroscopy. UV–vis absorption spectra were recorded on a Uvikon 933 spectrometer. Emission and excitation spectra were recorded on a Perkin-Elmer LS50B (working in the phosphorescence mode, with a microsecond delay time and 10 ms integration window) or on a PTI Quantamaster spectrometer. When necessary (Eu complexes), a Hamamatsu R928 photomultiplier was used. Luminescence decays were obtained on the PTI Quantamaster instrument over temporal windows covering at least five decay times. Luminescence quantum yields were measured according to conventional procedures,[48] with diluted solutions (optical density <0.05), using $[Ru(bipy)_3]Cl_2$ in nondegassed water ($\Phi = 2.8\%$),[49] rhodamine 6G in ethanol ($\Phi = 88\%$),[50] or a standard Tb complex ($\Phi = 31\%$ in H_2O)[28a] as references, with the necessary correction for refractive index of the media used.[65] Estimated errors are ±15%. Hydration numbers, q, were obtained using eq 1, where τ_{H_2O} and τ_{D_2O} respectively refer to the measured luminescence decay lifetimes (in ms) in water and deuterated water, using $A = 1.11$ and $B = 0.31$[14a] or $A = 1.2$ and $B = 0.25$[14c] for Eu and $A = 5$ and $B = 0.06$[14c] or $A = 4.2$ and $B = 0$[14b] for Tb (estimated error ±0.2 water molecules).

$$q = A(1/\tau_{H2O} - 1/\tau_{D2O} - B) \quad (1)$$

Computational Methods. All calculations were performed employing hybrid DFT with the B3LYP exchange-correlation functional[66] and the Gaussian 03 package (Revision C.01).[67] Full geometry optimizations of the $[Eu(\mathbf{L1'})(H_2O)_2]^+$, $[Eu(\mathbf{L2'})(H_2O)_2]^+$, and $[Eu(\mathbf{L3'})(H_2O)_2]^+$ systems were performed both in vacuo and in aqueous solution by using the 6-31G(d) basis set for C, H, N, and O atoms and the effective core potential (ECP) of Dolg et al. and the related [5s4p3d] GTO valence basis set for the lanthanides.[68] This ECP includes $46 + 4f^n$ electrons in the core, leaving the outermost 11 electrons to be treated explicitly. In these calculations the butyl groups of ligands **L1**−**L3** (Chart 1) were substituted by methyl groups, the methyl-substituted ligands being denoted as **L1′**−**L3′**, respectively. The stationary points found on the potential energy surfaces as a result of the geometry optimizations performed in vacuo have been tested to represent energy minima rather than saddle points via frequency analysis.

(61) Ruiz, J.; Ruiz Medel, M. J.; Daniel, M.-C.; Blais, J.-C.; Astruc, D. *Chem. Commun.* **2003**, 464–465.

(62) Bowman-James, K. *Acc. Chem. Res.* **2005**, *38*, 671–678.

(63) (a) Schäferling, M.; Wolfbeis, O. S. *Chem. Eur. J.* **2007**, *13*, 4342–4349. (b) Tremblay, M. S.; Zhu, Q.; Marti, A. A.; Dyer, J.; Halim, M.; Jockusch, S.; Turro, N. J.; Sames, D. *Org. Lett.* **2006**, *8*, 2723–2726. (c) Best, M. D.; Anslyn, E. V. *Chem. Eur. J.* **2003**, *9*, 51–57. (d) Li, S.-H.; Yu, C.-W.; Yuan, W.-T.; Xu, J.-G. *Anal. Sci.* **2004**, *20*, 1375–1377. (e) Li, S.-H.; Yuan, W.-T.; Zhu, C.-Q.; Xu, J.-G. *Anal. Biochem.* **2004**, *331*, 235–242.

(64) Gottlieb, H.; Kotlyar, V.; Nudelman, A. *J. Org. Chem.* **1997**, *62*, 7512–7515.

(65) Valeur, B. In *Molecular Fluorescence*; Wiley-VCH: Weinheim, Germany, 2002; p 161.

(66) (a) Becke, A. D. *J. Chem. Phys.* **1993**, *98*, 5648–5652. (b) Lee, C.; Yang; Parr, R. G. *Phys. Rev. B* **1988**, *37*, 785–789.

(67) Frisch, M. J.; Trucks, G. W.; Schlegel, H. B.; Scuseria, G. E.; Robb, M. A.; Cheeseman, J. R.; Montgomery, J. A. Jr.; Vreven, T.; Kudin, K. N.; Burant, J. C.; Millam, J. M.; Iyengar, S. S.; Tomasi, J.; Barone, V.; Mennucci, B.; Cossi, M.; Scalmani, G.; Rega, N.; Petersson, G. A.; Nakatsuji, H.; Hada, M.; Ehara, M.; Toyota, K.; Fukuda, R.; Hasegawa, J.; Ishida, M.; Nakajima, T.; Honda, Y.; Kitao, O.; Nakai, H.; Klene, M.; Li, X.; Knox, J. E.; Hratchian, H. P.; Cross, J. B.; Adamo, C.; Jaramillo, J.; Gomperts, R.; Stratmann, R. E.; Yazyev, O.; Austin, A. J.; Cammi, R.; Pomelli, C.; Ochterski, J. W.; Ayala, P. Y.; Morokuma, K.; Voth, G. A.; Salvador, P.; Dannenberg, J. J.; Zakrzewski, V. G.; Dapprich, S.; Daniels, A. D.; Strain, M. C.; Farkas, O.; Malick, D. K.; Rabuck, A. D.; Raghavachari, K.; Foresman, J. B.; Ortiz, J. V.; Cui, Q.; Baboul, A. G.; Clifford, S.; Cioslowski, J.; Stefanov, B. B.; Liu, G.; Liashenko, A.; Piskorz, P.; Komaromi, I.; Martin, R. L.; Fox, D. J.; Keith, T.; Al-Laham, M. A.; Peng, C. Y.; Nanayakkara, A.; Challacombe, M.; Gill, P. M. W.; Johnson, B.; Chen, W, Wong, M. W.; Gonzalez, C.; Pople, J. A. *Gaussian 03, Revision C.01*; Gaussian, Inc., Wallingford, CT, 2004.

(68) Dolg, M.; Stoll, H.; Savin, A.; Preuss, H. *Theor. Chim. Acta* **1989**, *75*, 173–194.

Solvent effects were evaluated by using the polarizable continuum model (PCM), in particular employing the integral equation formalism variant (IEF-PCM).[69] In line with the united atom topological model (UATM),[70] the solute cavity is built as an envelope of spheres centered on atoms or atomic groups with appropriate radii. For the Eu(III) ion, the previously parametrized radius was used.[71] To avoid convergence problems during geometry optimization, the linear search in the Berny algorithm was removed, and the nonelectrostatic contributions to the energy and energy gradient, viz., cavitation, dispersion, and repulsion contributions, were omitted. Owing to the slow convergence, the optimizations were stopped when the convergence parameters were about twice the default values.[72] For this reason frequency analysis was not performed to characterize the stationary points; thus, the final geometries correspond to stable conformations for the chosen minimization algorithm, rather than true minima. The in vacuo and in aqueous solution optimized Cartesian coordinates of the [Eu(**L1′**)$(H_2O)_2]^+$, [Eu(**L2′**)$(H_2O)_2]^+$, and [Eu(**L3′**)$(H_2O)_2]^+$ systems are given in the Supporting Information (Tables T1−T6).

Full geometry optimization and subsequent frequency analysis of the [Eu(**L2′**)$(MeTP)]^{3-}$ and [Eu(**L2′**)$(MeTP)(H_2O)]^{3-}$ systems were performed in vacuo by using the same combination of basis sets as described above. The relative stability of the [Eu(**L2′**)$(MeTP)]^{3-}$ and [Eu(**L2′**)$(MeTP)(H_2O)]^{3-}$ species was calculated as $\Delta G_{react} = G_{sol}([Eu(\mathbf{L2'})(MeTP)(H_2O)]^{3-}) - G_{sol}([Eu(\mathbf{L2'})(MeTP)]^{3-}) - G_{sol}(H_2O)$. The free energy in aqueous solution of each species (G_{sol}) was determined from solvated single-point energy calculations on the geometries optimized in vacuo (IEF-PCM). Non potential energy corrections (zero point energy and thermal terms) were obtained by frequency analysis in the gas phase. The in vacuo optimized Cartesian coordinates of the [Eu(**L2′**)$(MeTP)]^{3-}$ and [Eu(**L2′**)$(MeTP)(H_2O)]^{3-}$ systems are given in the Supporting Information (Tables T7 and T8).

Synthesis of the Ligands. Synthesis of Compound 2. A solution of **1** (1 g, 3.07 mmol), AIBN (101 mg, 0.61 mmol), and NBS (2.73 g, 15.3 mmol) in benzene (90 mL) was heated at reflux with a standard 100 W halogen lamp for 20 h. The solvent was then removed under reduced pressure, and the residue, consisting of a mixture of **1**, the monobromo derivative **3**, and the corresponding gem-dibrominated analogue **2**, was purified by column chromatography (SiO_2, CH_2Cl_2/hexane 80/20 to 100/0; $R_f = 0.56$, Al_2O_3, CH_2Cl_2/cyclohexane 30/70). Yield: 969 mg (65%), white crystalline powder. IR (solid): 1562 (m), 1548 (m), 1423 (s), 1127 (m), 788 (s) cm^{-1}. ^1H NMR ($CDCl_3$): δ 6.77 (s, 1H), 7.51 (d, 1H, $^3J = 8.0$ Hz), 7.71 (t, 1H, $^3J = 8.0$ Hz), 7.85 (dd, 1H, $^3J = 8.0$ Hz, $^4J = 1.0$ Hz), 7.95 (t, 1H, $^3J = 8.0$ Hz), 7.96 (t, 1H, $^3J = 8.0$ Hz), 8.46 (dd, 1H, $^3J = 8.0$ Hz, $^4J = 1.0$ Hz), 8.51 (d, 1H, $^3J = 8.0$ Hz), 8.53 (d, 1H, $^3J = 8.0$ Hz), 8.55 (d, 1H, $^3J = 8.0$ Hz). $^{13}C\{^1H\}$ NMR ($CDCl_3$): δ 41.8, 119.7, 121.3, 121.8, 121.9, 122.0, 128.1, 138.1, 138.5, 139.1, 141.6, 153.7, 154.4, 154.5, 157.2, 158.4. MS (FAB^+): *m/z* 484.2 ($[M + H]^+$, 100%), 486.2 ($[M + H]^+$, 98%). Anal. Calcd for $C_{16}H_{10}Br_3N_3$: C, 39.71; H, 2.08; N, 8.68. Found: C, 39.44; H, 1.84; N, 8.40.

Synthesis of Compound 4. A Schlenk tube under argon was successively charged with **2** (410 mg, 0.85 mmol), *n*-butylamine (500 μL, 5.1 mmol), and anhydrous K_2CO_3 (468 mg, 3.39 mmol) in 10 mL of dry acetonitrile. The resulting suspension was heated to 80 °C over 26 h. The mixture was evaporated to dryness, 45 mL of CH_2Cl_2 and 25 mL of water were added, and the aqueous phase was extracted once with 30 mL of CH_2Cl_2. The combined organic layers were dried over $MgSO_4$, filtered, and evaporated to dryness to give the intermediate imine. Yield: 334 mg (99%), yellow-orange solid. IR (solid): 2952 (w), 2929 (w), 2856 (w), 1650 (w), 1570 (m), 1551 (s), 1424 (s), 1134 (m), 786 (s) cm^{-1}. ^1H NMR ($CDCl_3$): δ 0.98 (t, 3H, $^3J = 7.0$ Hz), 1.37–1.50 (m, 2H), 1.69–1.79 (m, 2H), 3.72 (td, 2H, $^3J = 7.0$ Hz, $^4J = 1.0$ Hz), 7.52 (dd, 1H, $^3J = 8.0$ Hz, $^4J = 1.0$ Hz), 7.71 (t, 1H, $^3J = 8.0$ Hz), 7.90 (t, 1H, $^3J = 8.0$ Hz), 7.97 (t, 1H, $^3J = 8.0$ Hz), 8.07 (dd, 1H, $^3J = 8.0$ Hz, $^4J = 1.0$ Hz), 8.46 (dd, 1H, $^3J = 8.0$ Hz, $^4J = 1.0$ Hz), 8.49 (s, 1H), 8.55 (dd, 1H, $^3J = 8.0$ Hz, $^4J = 1.0$ Hz), 8.59 (dd, 1H, $^3J = 8.0$ Hz, $^4J = 1.0$ Hz), 8.60 (dd, 1H, $^3J = 8.0$ Hz, $^4J = 1.0$ Hz). $^{13}C\{^1H\}$ NMR ($CDCl_3$): δ 13.9, 20.5, 32.8, 61.3, 119.8, 121.0, 121.5, 121.6, 121.9, 128.0, 137.3, 138.0, 139.1, 141.6, 153.7, 154.3, 155.1, 155.5, 157.4, 162.2. MS (FAB^+): *m/z* 395.2 ($[M + H]^+$, 100%), 397.1 ($[M + H]^+$, 100%). Anal. Calcd for $C_{20}H_{19}BrN_4$: C, 60.77; H, 4.84; N, 14.17. Found: C, 60.54; H, 4.66; N, 13.76.

A Schlenk tube under argon was charged with the intermediate imine (295 mg, 0.75 mmol) and $NaBH_4$ (169 mg, 4.48 mmol) in 10 mL of ethanol. The resulting solution was heated to 65 °C for 35 h. A few drops of water were carefully added, and the mixture was evaporated to dryness. The compound was extracted with CH_2Cl_2 and the resulting solution dried with $MgSO_4$, filtered, and evaporated to dryness. Compound **4** (295 mg, 99%) was isolated as an orange powder. IR (solid): 2952 (w), 2927 (w), 2969 (w), 1568 (s), 1549 (s), 1422 (s), 1129 (s), 1071 (m), 782 (s) cm^{-1}. ^1H NMR ($CDCl_3$): δ 0.92 (t, 3H, $^3J = 7.0$ Hz), 1.36–1.44 (m, 2H), 1.54–1.63 (m, 2H), 2.74 (t, 2H, $^3J = 7.0$ Hz), 4.01 (s, 2H), 7.34 (d, 1H, $^3J = 7.0$ Hz), 7.50 (dd, 1H, $^3J = 8.0$ Hz, $^4J = 1.0$ Hz), 7.70 (t, 1H, $^3J = 8.0$ Hz), 7.80 (t, 1H, $^3J = 8.0$ Hz), 7.94 (t, 1H, $^3J = 8.0$ Hz), 8.44 (dd, 1H, $^3J = 8.0$ Hz, $^4J = 1.0$ Hz), 8.45 (d, 1H, $^3J = 8.0$ Hz), 8.51 (dd, 1H, $^3J = 8.0$ Hz, $^4J = 1.0$ Hz), 8.58 (dd, 1H, $^3J = 8.0$ Hz, $^4J = 1.0$ Hz). $^{13}C\{^1H\}$ NMR ($CDCl_3$): δ 14.0, 20.5, 32.2, 49.3, 55.0, 119.3, 119.8, 121.3, 121.6, 122.4, 127.9, 137.2, 137.9, 139.1, 141.5, 153.6, 155.4, 155.5, 157.4, 158.9. MS (FAB^+): *m/z* 397.2 ($[M + H]^+$, 100%), 399.1 ($[M + H]^+$, 100%). Anal. Calcd for $C_{20}H_{21}BrN_4$: C, 60.46; H, 5.33; N, 14.10. Found: C, 60.22; H, 5.18; N, 13.70.

Synthesis of Compound 6. A Schlenk tube under argon was successively charged with compound **4** (100 mg, 0.25 mmol), 6-carboethoxy-6′-(bromomethyl)bipyridine (**5**; 71 mg, 0.29 mmol), and K_2CO_3 (120 mg, 0.87 mmol) in dry CH_3CN (10 mL). The resulting mixture was heated to 80 °C over 27 h. The CH_3CN was removed under reduced pressure, resulting in the recovery of an orange solid, which was then purified by column chromatography (Al_2O_3; CH_2Cl_2) to give compound **6** ($R_f = 0.40$, Al_2O_3, CH_2Cl_2, 141 mg, 87%), as a pale yellow crystalline solid. IR (solid): 2958 (w), 2919 (w), 2815 (w), 1533 (s), 1571 (s), 1551 (s), 1426 (s), 1293 (m), 1267 (s), 1226 (s), 1153 (s), 1132 (m), 782 (s), 774 (s) cm^{-1}. ^1H NMR ($CDCl_3$): δ 0.86 (t, 3H, $^3J = 7.0$ Hz), 1.26–1.38 (m, 2H), 1.42 (t, 3H, $^3J = 7.0$ Hz), 1.54–1.61 (m, 2H), 2.61 (t, 2H, $^3J = 7.0$ Hz), 3.92 (s, 2H), 4.01 (s, 2H), 4.46 (q, 2H, $^3J = 11.0$ Hz), 7.50 (d, 1H, $^3J = 8.0$ Hz), 7.55 (d, 1H, $^3J = 8.0$ Hz), 7.70 (t, 1H, $^3J = 8.0$ Hz), 7.78 (d, 1H, $^3J = 8.0$ Hz), 7.82 (d, 1H, $^3J = 8.0$ Hz), 7.87 (d, 1H, $^3J = 8.0$ Hz), 7.93 (d, 1H, $^3J = 8.0$ Hz), 7.97 (d, 1H, $^3J = 7.0$ Hz), 8.41–8.45 (m, 2H), 8.49 (d, 1H, $^3J = 8.0$ Hz), 8.58 (d, 1H, $^3J = 8.0$ Hz). $^{13}C\{^1H\}$ NMR ($CDCl_3$): δ 14.0, 14.3, 20.5, 29.6, 54.4, 60.4, 60.5, 61.8, 119.1, 119.8, 121.2, 121.7, 122.9,

(69) (a) Cancès, M. T.; Mennucci, B.; Tomasi, J. *J. Chem. Phys.* **1997**, *107*, 3032–3041. (b) Mennucci, B.; Tomasi, J. *J. Chem. Phys.* **1997**, *106*, 5151–5158. (c) Mennucci, B.; Cancès, E.; Tomasi, J. *J. Phys. Chem. B* **1997**, *101*, 10506–10517. (d) Tomasi, J.; Mennucci, B.; Cancès, E. *THEOCHEM* **1999**, *464*, 211–226.

(70) Barone, V.; Cossi, M.; Tomasi, J. *J. Chem. Phys.* **1997**, *107*, 3210–3221.

(71) Cosentino, U.; Villa, A.; Pitea, D.; Moro, G.; Barone, V. *J. Phys. Chem. B* **2000**, *104*, 8001–8007.

(72) Cosentino, U.; Moro, G.; Pitea, D.; Barone, V.; Villa, A.; Muller, R. N.; Botteman, F. *Theor. Chem. Acc.* **2004**, *111*, 204–209.

123.3, 125.7, 127.9, 137.08, 137.11, 137.9, 139.1, 141.5, 147.6, 153.6, 155.2, 155.7, 157.5, 159.4, 161.5, 165.4. MS (FAB$^+$): *m/z* 560.1 ([M + H]$^+$, 100%), 562.1 ([M + H]$^+$, 80%). Anal. Calcd for $C_{29}H_{30}BrN_5O_2$: C, 62.14; H, 5.39; N, 12.49. Found: C, 61.86; H, 5.21; N, 12.21.

Synthesis of Ligand L1H$_2$. A solution of **6** (123 mg, 0.22 mmol) and [Pd(PPh$_3$)$_2$Cl$_2$] (15.4 mg, 0.022 mmol) in a mixture of EtOH (25 mL) and Et$_3$N (25 mL) was heated to 70 °C for 19 h under a continuous flow of CO. The resulting solution was evaporated to dryness, the residue was dissolved in CH_2Cl_2 (25 mL), and this solution was filtered and extracted by addition of water (10 mL). After the aqueous layer was washed with CH_2Cl_2 (20 mL) and the combined organic layers were dried ($MgSO_4$), filtered, and evaporated to dryness, a yellowish residue was obtained which, after purification by column chromatography (Al_2O_3; CH_2Cl_2), gave the intermediate ethyl ester (R_f = 0.63, Al_2O_3, CH_2Cl_2/MeOH 99/1, 98 mg, 80%) as a yellowish solid. IR (CH_2Cl_2): 2951 (w), 2930 (w), 2869 (w), 2821 (w), 1734 (s), 1714 (s), 1578 (s), 1569 (s), 1433 (s), 1369 (m), 1310 (s), 1268 (s), 1237 (s), 1134 (s), 1075 (s), 773 (s), 761 (s) cm^{-1}. ^{1}H NMR ($CDCl_3$): δ 0.85 (t, 3H, ^3J = 7.0 Hz), 1.24–1.35 (m, 2H), 1.41 (t, 3H, ^3J = 7.0 Hz), 1.47 (t, 3H, ^3J = 7.0 Hz), 1.52–1.62 (m, 2H), 2.60 (t, 2H, ^3J = 7.0 Hz), 3.91 (s, 2H), 4.0 (s, 2H), 4.45 (q, 2H, ^3J = 11.0 Hz), 4.50 (q, 2H, ^3J = 11.0 Hz), 7.54 (t, 1H, ^3J = 7.0 Hz), 7.78 (d, 1H, ^3J = 7.0 Hz), 7.82 (d, 1H, ^3J = 7.0 Hz), 7.87 (d, 1H, ^3J = 7.0 Hz), 7.92–7.98 (m, 2H), 7.97 (t, 1H, ^3J = 8.0 Hz), 8.13 (dd, 1H, ^3J = 8.0 Hz, ^4J = 1.0 Hz), 8.44 (d, 1H, ^3J = 8.0 Hz), 8.49 (dd, 1H, ^3J = 8.0 Hz, ^4J = 1.0 Hz), 8.58 (dd, 1H, ^3J = 8.0 Hz, ^4J = 1.0 Hz), 8.80 (dd, 1H, ^3J = 8.0 Hz, ^4J = 1.0 Hz). ^{13}C{^{1}H} NMR ($CDCl_3$): δ 14.0, 14.3, 20.4, 29.5, 54.3, 60.4, 61.7, 61.8, 119.1, 121.4, 121.5, 122.8, 123.2, 124.1, 124.8, 125.7, 137.0, 137.1, 137.6, 137.9, 147.5, 147.8, 154.3, 155.2, 155.5, 156.4, 159.3, 161.4, 165.3, 165.4. MS (FAB$^+$): *m/z* 508.2 ([M − OEt]$^+$, 20%), 554.2 ([M + H]$^+$, 100%). Anal. Calcd for $C_{32}H_{35}N_5O_4$: C, 69.42; H, 6.37; N, 12.65. Found: C, 69.32; H, 6.19; N, 12.44.

The intermediate ethyl ester (80 mg, 145 μmol) was dissolved in concentrated HCl (14 mL) and heated to 80 °C over 63 h. After the mixture had cooled to room temperature, the solvent was evaporated under reduced pressure. The solid was recrystallized with MeOH/Et$_2$O to give the title ligand **L1**H$_2$. Yield: 67.1 mg, 70%, orange crystalline solid. IR (solid): 3376 (s), 2962 (w), 2875 (w), 1722 (s), 1615 (m), 1589 (s), 1434 (s), 1347 (s), 1265 (s), 1175 (m), 996 (m), 767 (s) cm^{-1}. ^{1}H NMR (CD_3OD): δ 0.96 (t, 3H, ^3J = 7.0 Hz), 1.42–1.52 (m, 2H), 1.9–2.0 (m, 2H), 3.53 (t, 2H, ^3J = 8.0 Hz), 4.90 (s, 2H), 4.91 (s, 2H), 7.67 (d, 1H, ^3J = 7.0 Hz), 7.72 (d, 1H, ^3J = 8.0 Hz), 7.97 (d, 1H, ^3J = 8.0 Hz), 8.03 (t, 1H, ^3J = 7.0 Hz), 8.13 (t, 1H, ^3J = 8.0 Hz), 8.28–8.32 (m, 2H), 8.39 (t, 1H, ^3J = 8.0 Hz), 8.60 (d, 1H, ^3J = 8.0 Hz), 8.72 (d, 1H, ^3J = 8.0 Hz), 8.78 (d, 1H, ^3J = 8.0 Hz), 8.80 (d, 1H, ^3J = 8.0 Hz). ^{13}C{^{1}H} NMR (CD_3OD): δ 13.9, 20.9, 27.0, 57.2, 58.9, 59.0, 123.4, 124.5, 124.6, 126.3, 126.6, 127.1, 127.7, 128.1, 140.6, 140.8, 141.6, 143.8, 148.6, 148.7, 151.8, 152.1, 152.3, 153.0, 153.05, 153.2, 166.7, 167.2. MS (FAB$^+$): *m/z* 497.2 ([M]$^+$, 100%). Anal. Calcd for $C_{28}H_{27}N_5O_4 \cdot 3HCl \cdot 3H_2O$: C, 50.88; H, 5.49; N, 10.60. Found: C, 50.43; H, 5.68; N, 10.55.

Synthesis of Compound 8. A Schlenk tube under argon was successively charged with compound **4** (250 mg, 0.63 mmol), compound **7** (248 mg, 0.76 mmol), and K_2CO_3 (260 mg, 1.89 mmol) in dry CH_3CN (15 mL). The resulting mixture was heated to 80 °C over 58 h. The CH_3CN was removed under reduced pressure, resulting in the recovery of an orange solid, which was then purified by column chromatography (Al_2O_3; CH_2Cl_2/cyclohexane 80/20 to 100/0) to give compound **8** (R_f = 0.67, Al_2O_3, CH_2Cl_2/cyclohexane 80/20, 403 mg, 82%) as a deep orange solid. IR (solid): 2949 (w), 2922 (w), 2822 (w), 1571 (s), 1548 (s), 1419 (s), 1126 (s), 1073 (m), 789 (s), 779 (s) cm^{-1}. ^{1}H NMR ($CDCl_3$): δ 0.88 (t, 3H, ^3J = 7.0 Hz), 1.29–1.43 (m, 2H), 1.58–1.64 (m, 2H), 2.64 (t, 2H, ^3J = 7.0 Hz), 3.94 (s, 2H), 3.96 (s, 2H), 7.44 (d, 1H, ^3J = 8.0 Hz), 7.49 (d, 1H, ^3J = 8.0 Hz), 7.58–7.62 (m, 3H), 7.69 (t, 1H, ^3J = 8.0 Hz), 7.76 (d, 1H, ^3J = 8.0 Hz), 7.82 (t, 1H, ^3J = 8.0 Hz), 7.91 (t, 1H, ^3J = 8.0 Hz), 8.24 (d, 1H, ^3J = 8.0 Hz), 8.38–8.42 (m, 3H), 8.48 (d, 1H, ^3J = 8.0 Hz), 8.56 (d, 1H, ^3J = 8.0 Hz). ^{13}C{^{1}H} NMR ($CDCl_3$): δ 14.0, 20.5, 29.6, 54.3, 60.4, 60.5, 119.1, 119.4, 119.7, 121.1, 121.6, 122.9, 123.3, 127.7, 127.9, 137.0, 137.2, 137.8, 139.0, 139.1, 141.4, 141.5, 153.5, 153.5, 155.0, 155.7, 157.4, 157.6, 159.7, 159.9. MS (FAB$^+$): *m/z* 643.2 ([M + H]$^+$, 50%), 645.2 ([M + H]$^+$, 100%), 647.1 ([M + H]$^+$, 55%). Anal. Calcd for $C_{31}H_{28}Br_2N_6$: C, 57.78; H, 4.38; N, 13.04. Found: C, 57.55; H, 4.20; N, 12.70.

Synthesis of L2H$_2$. A solution of **8** (300 mg, 0.47 mmol) and [Pd(PPh$_3$)$_2$Cl$_2$] (52 mg, 74 μmol) in a mixture of EtOH (50 mL) and Et$_3$N (50 mL) was heated to 70 °C for 41 h under a CO atmosphere. The resulting solution was evaporated to dryness, the residue was dissolved in CH_2Cl_2 (25 mL), and this solution was filtered and extracted by addition of water (10 mL). After the aqueous layer was washed with CH_2Cl_2 (20 mL) and the combined organic layers were dried ($MgSO_4$), filtered, and evaporated to dryness, a yellowish residue was obtained which, after purification by column chromatography (Al_2O_3; CH_2Cl_2), give the intermediate ethyl ester (R_f = 0.73, Al_2O_3, CH_2Cl_2/MeOH 99.5/0.5, 262 mg, 89%) as a milky oil. IR (CH_2Cl_2): 2956 (w), 2931 (w), 2868 (w), 1739 (m), 1717 (s), 1579 (s), 1566 (s), 1434 (s), 1136 (s), 769 (s) cm^{-1}. ^{1}H NMR (CD_3OD): δ 0.86 (t, 3H, ^3J = 7.0 Hz), 1.30–1.38 (m, 2H), 1.45 (t, 3H, ^3J = 7.0 Hz), 1.47 (t, 3H, ^3J = 7.0 Hz), 1.55–1.71 (m, 2H), 2.64 (t, 2H, ^3J = 7.0 Hz), 3.95 (s, 2H), 3.96 (s, 2H), 4.47 (q, 2H, ^3J = 10.0 Hz), 4.50 (q, 2H, ^3J = 10.0 Hz), 7.59–7.63 (m, 2H), 7.79–7.83 (m, 2H), 7.88 (d, 1H, ^3J = 8.0 Hz), 7.92 (d, 1H, ^3J = 8.0 Hz), 7.98 (d, 1H, ^3J = 8.0 Hz), 8.07 (dd, 1H, ^3J = 8.0 Hz, ^4J = 1.0 Hz), 8.12 (dd, 1H, ^3J = 8.0 Hz, ^4J = 1.0 Hz), 8.42 (t, 2H, ^3J = 8.0 Hz), 8.50 (dd, 1H, ^3J = 8.0 Hz, ^4J = 1.0 Hz), 8.58 (dd, 1H, ^3J = 8.0 Hz, ^4J = 1.0 Hz), 8.62 (dd, 1H, ^3J = 8.0 Hz, ^4J = 1.0 Hz), 8.79 (dd, 1H, ^3J = 8.0 Hz, ^4J = 1.0 Hz). ^{13}C{^{1}H} NMR (CD_3OD): δ 14.0, 14.3, 20.5, 29.5, 53.4, 54.3, 60.4, 60.4, 61.7, 61.8, 119.1, 119.6, 121.3, 121.5, 122.8, 123.2, 124.1, 124.1, 124.6, 124.8, 137.0, 137.2, 137.6 (2C), 137.8, 147.6, 147.7, 154.3, 155.1, 155.6, 156.4, 156.6, 159.7, 165.3. MS (FAB$^+$): *m/z* 557.1 ([M − $C_3H_5O_2$]$^+$, 20%), 631.2 ([M + H]$^+$, 100%). Anal. Calcd for $C_{37}H_{38}N_6O_4$: C, 70.46; H, 6.07; N, 13.32. Found: C, 70.30; H, 5.82; N, 13.25.

The intermediate ester (160 mg, 260 μmol) was dissolved in concentrated HCl (16 mL) and heated to 80 °C over 144 h. After the mixture had cooled to room temperature, the solvent was evaporated under reduced pressure. The solid was recrystallized with MeOH-/Et$_2$O to give **L2**H$_2$. Yield: 157 mg, 95%, yellowish crystalline solid. IR (solid): 3369 (s), 2960 (w), 2866 (w), 1713 (s), 1615 (m), 1580 (s), 1568 (s), 1435 (s), 1349 (s), 1222 (m), 1146 (s), 807 (s), 770 (s) cm^{-1}. ^{1}H NMR ($CDCl_3$): δ 0.99 (t, 3 H, ^3J = 7.0 Hz), 1.44–1.52 (m, 2H), 1.93–2.04 (m, 2H), 3.61 (t, 2H, ^3J = 7.0 Hz), 4.99 (s, 2H), 5.00 (s, 2H), 7.53 (d, 1H, ^3J = 8.0 Hz), 7.69 (d, 1H, ^3J = 8.0 Hz), 7.72 (d, 1H, ^3J = 8.0 Hz), 7.94 (t, 1H, ^3J = 8.0 Hz), 8.03 (dd, 1H, ^3J = 7.0 Hz, ^4J = 1.0 Hz), 8.12 (t, 1H, ^3J = 8.0 Hz), 8.21 (d, 1H, ^3J = 8.0 Hz), 8.26 (d, 1H, ^3J = 8.0 Hz), 8.32 (dd, 1H, ^3J = 8.0 Hz, ^4J = 2.0 Hz), 8.39 (d, 1H, ^3J = 8.0 Hz), 8.43 (d, 1H, ^3J = 8.0 Hz), 8.53 (d, 1H, ^3J = 8.0 Hz), 8.62 (d, 1H, ^3J = 7.0 Hz), 8.67 (d, 1H, ^3J = 7.0 Hz), 8.68 (d, 1H, ^3J = 7.0 Hz). ^{13}C{^{1}H} NMR ($CDCl_3$): δ 13.8, 20.9, 27.3, 57.7, 59.4, 59.5,

123.2, 123.3, 123.4, 123.7, 123.8, 125.5, 125.7, 126.0, 126.2, 126.4, 127.1, 139.4, 140.3, 140.4, 140.7, 140.8, 141.9 148.7, 149.0, 151.4, 151.6, 156.3, 156.4, 166.9. MS (FAB^+): *m/z* 575.2 ($[M + H]^+$, 100%). Anal. Calcd for $C_{33}H_{30}N_6O_4 \cdot HCl \cdot 2H_2O$: C, 61.25; H, 5.45; N, 12.99. Found: C, 61.10; H, 5.33; N, 12.74.

Synthesis of Compound 9. A Schlenk tube under argon was successively charged with compound **4** (100 mg, 0.25 mmol), **3** (117 mg, 0.29 mmol), and K_2CO_3 (120 mg, 0.87 mmol) in dry CH_3CN (10 mL). The mixture was heated to 80 °C over 93 h. The CH_3CN was removed under reduced pressure, resulting in the recovery of an orange solid, which was then purified by column chromatography (Al_2O_3; CH_2Cl_2) to give compound **9** ($R_f = 0.63$, Al_2O_3, CH_2Cl_2, 183 mg, 87%), as a white crystalline solid. IR (solid): 2949 (w), 2926 (w), 2867 (w), 2817 (w), 1568 (s), 1548 (s), 1421 (s), 1126 (m), 1074 (m), 780 (s) cm^{-1}. ^1H NMR ($CDCl_3$): δ 0.89 (t, 3H, $^3J = 7.0$ Hz), 1.28–1.41 (m, 2H), 1.59–1.66 (m, 2H), 2.67 (t, 2H, $^3J = 7.0$ Hz), 3.98 (s, 4H), 7.50 (dd, 2H, $^3J = 8.0$ Hz, $^4J = 1.0$ Hz), 7.63 (d, 2H, $^3J = 8.0$ Hz), 7.69 (t, 2H, $^3J = 8.0$ Hz), 7.82 (t, 2H, $^3J = 8.0$ Hz), 7.91 (t, 2H, $^3J = 8.0$ Hz), 8.38–8.44 (m, 4H), 8.49 (dd, 2H, $^3J = 8.0$ Hz, $^4J = 1.0$ Hz), 8.57 (dd, 2H, $^3J = 8.0$ Hz, $^4J = 1.0$ Hz). $^{13}C\{^1H\}$ NMR ($CDCl_3$): δ 14.1, 20.5, 29.6, 54.4, 60.5, 119.1, 119.8, 121.2, 121.7, 122.9, 127.9, 137.1, 137.9, 139.1, 141.5, 153.6, 155.1, 155.7, 157.5, 159.8. MS (FAB^+): *m/z* 720.1 ($[M + H]^+$, 50%), 722.1 ($[M + H]^+$, 100%), 724.1 ($[M + H]^+$, 60%). Anal. Calcd for $C_{36}H_{31}Br_2N_7$: C, 59.93; H, 4.33; N, 13.59. Found: C, 59.72; H, 4.12; N, 13.30.

Synthesis of L3H$_2$. A solution of **9** (160 mg, 0.22 mmol) and $[Pd(PPh_3)_2Cl_2]$ (15.6 mg, 22 μmol) in a mixture of EtOH (40 mL) and Et_3N (40 mL) was heated at 70 °C for 25 h under a CO atmosphere. The resulting solution was evaporated to dryness, the residue was dissolved in CH_2Cl_2 (25 mL), and this solution was filtered and extracted by addition of water (10 mL). After the aqueous layer was washed with CH_2Cl_2 (20 mL) and the combined organic layers were dried ($MgSO_4$), filtered, and evaporated to dryness, a yellowish residue was obtained which, after purification by column chromatography (Al_2O_3; CH_2Cl_2/cyclohexane: 50/50 to 100/0) gave the intermediate ethyl ester ($R_f = 0.76$, Al_2O_3, CH_2Cl_2/MeOH 99/1) as a white solid (147 mg, 94%). IR (CH_2Cl_2): 2955 (w), 2929 (w), 2870 (w), 2815 (w), 1735 (s), 1713 (s), 1567 (s), 1434 (s), 1310 (m), 1258 (s), 1235 (s), 1129 (s), 1074 (s), 992 (m), 798 (s), 766 (s) cm^{-1}. ^1H NMR ($CDCl_3$): δ 0.89 (t, 3H, $^3J = 7.0$ Hz), 1.33–1.40 (m, 2H), 1.48 (t, 6H, $^3J = 7.0$ Hz), 1.59–1.67 (m, 2H), 2.67 (t, 2H, $^3J = 7.0$ Hz), 3.99 (s, 4H), 4.51 (q, 4H, $^3J = 11.0$ Hz), 7.63 (d, 2H, $^3J = 7.0$ Hz), 7.83 (t, 2H, $^3J = 8.0$ Hz), 7.93 (d, 2H, $^3J = 8.0$ Hz), 7.99 (d, 2H, $^3J = 8.0$ Hz), 8.13 (dd, 2H, $^3J = 8.0$ Hz, $^4J = 1.0$ Hz), 8.45 (d, 2H, $^3J = 8.0$ Hz), 8.52 (dd, 2H, $^3J = 8.0$ Hz, $^4J = 1.0$ Hz), 8.59 (dd, 2H, $^3J = 8.0$ Hz, $^4J = 1.0$ Hz), 8.81 (dd, 2H, $^3J = 8.0$ Hz, $^4J = 1.0$ Hz). $^{13}C\{^1H\}$ NMR ($CDCl_3$): δ 14.1, 14.3, 20.5, 29.6, 54.3, 60.4, 61.8, 119.1, 121.4, 121.6, 122.9, 124.1, 124.8, 137.1, 137.7, 137.9, 147.8, 154.3, 155.1, 155.6, 156.5, 159.8, 165.3. MS (FAB^+): *m/z* 708.2 ($[M + H]^+$, 100%). Anal. Calcd for $C_{42}H_{41}N_7O_4$: C, 71.27; H, 5.84; N, 13.85. Found: C, 70.94; H, 5.67; N, 13.69.

The intermediate ethyl ester (110 mg, 155 μmol) was dissolved in concentrated HCl (18 mL) and heated to 80 °C over 63 h. After the mixture had cooled to room temperature, the solvent was evaporated under reduced pressure. The solid was recrystallized with MeOH/Et_2O to give **L3**H_2 (111 mg, 87%) as a pale orange crystalline solid. IR (solid): 3361 (s), 3067 (w), 2961 (w), 2874 (w), 1722 (s), 1615 (s), 1587 (s), 1568 (s), 1434 (s), 1349 (s), 1271 (s), 1225 (s), 1171 (m), 1147 (s), 994 (m), 805 (s), 767 (s) cm^{-1}. ^1H NMR (CD_3OD): δ 0.98 (t, 3H, $^3J = 7.0$ Hz), 1.44–1.54 (m, 2H), 1.96–2.06 (m, 2H), 3.67 (t, 2H, $^3J = 8.0$ Hz), 5.08 (s, 4H), 7.72 (d, 2H, $^3J = 8.0$ Hz), 8.07 (t, 2H, $^3J = 8.0$ Hz), 8.12–8.16 (m, 2H), 8.23 (d, 2H, $^3J = 8.0$ Hz), 8.29 (dd, 2H, $^3J = 8.0$ Hz, $^4J = 1.0$ Hz), 8.37 (d, 2H, $^3J = 8.0$ Hz), 8.46 (d, 2H, $^3J = 8.0$ Hz), 8.52–8.58 (m, 4H). $^{13}C\{^1H\}$ NMR (CD_3OD): δ 13.9, 21.0, 27.1, 57.7, 59.3, 123.7, 124.5, 124.8, 126.6, 126.9, 128.0, 140.9, 141.8, 143.9, 148.4, 151.5, 151.8, 152.3, 152.7, 152.9, 166.6. MS (FAB^+): *m/z* 652.2 ($[M]^+$, 100%). Anal. Calcd for $C_{38}H_{33}N_7O_4 \cdot 3HCl \cdot 3H_2O$: C, 55.99; H, 5.19; N, 12.03. Found: C, 56.19; H, 5.05; N, 11.92.

Synthesis of the Complexes. Synthesis of [Eu(L1)(H$_2$O)$_2$]Cl·2H$_2$O. A solution of $EuCl_3 \cdot 6H_2O$ (8.3 mg, 22.6 μmol) in MeOH (10 mL) was added to a solution of ligand **L1**H_2 (15.0 mg, 22.7 μmol) in a mixture of 10 mL of MeOH and 3 mL of H_2O. The resulting mixture was agitated for 16 h at 70 °C. After addition of triethylamine (14 μL, 102 μmol) and an additional 3 h of agitation at room temperature, the solution was concentrated in vacuo. Addition of Et_2O led to the precipitation of the desired complex, which was isolated by centrifugation and dried under vacuum. Yield: 16.7 mg (97%), orange crystalline powder. IR (solid): 3361 (s), 3074 (w), 2961 (w), 2872 (w), 1620 (m), 1590 (s), 1572 (s), 1455 (m), 1378 (m), 1014 (m), 776 (m) cm^{-1}. MS (FAB^+): *m/z* 646.2 ($[Eu(\mathbf{L1})]^+$, 70%). Anal. Calcd for $C_{28}H_{25}ClN_5O_4Eu \cdot 4H_2O$: C, 44.54; H, 4.41; N, 9.28. Found: C, 44.39; H, 4.20; N, 9.02.

Synthesis of [Tb(L1)(H$_2$O)$_2$]Cl·H$_2$O. A solution of $TbCl_3 \cdot 6H_2O$ (5.6 mg, 15.0 μmol) in MeOH (10 mL) was added to a solution of ligand **L1**H_2 (10.0 mg, 15.1 μmol) in a mixture of 10 mL of MeOH and 3 mL of H_2O. The resulting mixture was agitated for 16 h at 70 °C. After addition of triethylamine (9.5 μL, 68 μmol) and an additional 3 h of agitation at room temperature, the solution was concentrated in vacuo. Addition of Et_2O led to the precipitation of the desired complex, which was isolated by centrifugation and dried under vacuum. Yield: 10.8 mg (96%), yellowish powder. IR (solid): 3386 (s), 3070 (w), 2960 (w), 2872 (w), 1640 (m), 1594 (s), 1573 (s), 1454 (m), 1375 (m), 1349 (m), 1014 (m), 777 (m) cm^{-1}. MS (FAB^+): *m/z* 654.1 ($[Tb(\mathbf{L1})]^+$, 80%). Anal. Calcd for $C_{28}H_{25}ClN_5O_4Tb \cdot 3H_2O$: C, 45.20; H, 4.20; N, 9.41. Found: C, 45.07; H, 3.82; N, 9.19.

Synthesis of [Eu(L2)(H$_2$O)$_2$]Cl·H$_2$O. A solution of $EuCl_3 \cdot 6H_2O$ (11.3 mg, 30.8 μmol) in MeOH (10 mL) was added to a solution of ligand **L2**H_2 (20.0 mg, 30.9 μmol) in a mixture of 10 mL of MeOH and 3 mL of H_2O. The resulting mixture was agitated for 18 h at 70 °C. After addition of triethylamine (17 μL, 124 μmol) and an additional 3 h of agitation at room temperature, the solution was concentrated in vacuo. Addition of Et_2O led to the precipitation of the desired complex, which was isolated by centrifugation and dried under vacuum. Yield: 21.6 mg (86%), yellowish crystalline powder. IR (solid): 3390 (s), 1614 (s), 1591 (s), 1572 (s), 1461 (m), 1373 (m), 1011 (m), 778 (m) cm^{-1}. MS (FAB^+): *m/z* 723.2 ($[Eu(\mathbf{L2})]^+$, 85%), 725.2 ($[Eu(\mathbf{L2})]^+$, 100%). Anal. Calcd for $C_{33}H_{28}N_6O_4Eu \cdot Cl \cdot 3H_2O$: C, 48.69; H, 4.21; N, 10.32. Found: C, 48.44; H, 3.84; N, 10.16.

Synthesis of [Tb(L2)(H$_2$O)$_2$]Cl·H$_2$O. A solution of $TbCl_3 \cdot 6H_2O$ (8.7 mg, 23 μmol) in MeOH (10 mL) was added to a solution of ligand **L2**H_2 (15.0 mg, 23 μmol) in a mixture of 10 mL of MeOH and 3 mL of H_2O. The resulting mixture was agitated for 16 h at 70 °C. After addition of triethylamine (13 μL, 93 μmol) and an additional 3 h of agitation at room temperature, the solution was concentrated in vacuo. Addition of Et_2O led to the precipitation of the desired complex, which was isolated by centrifugation and dried under vacuum. Yield: 18.6 mg (98%), yellowish crystalline powder. IR (solid): 3381 (s), 2960 (w), 1615 (s), 1592 (s), 1574 (s), 1463 (m), 1391 (m),

1011 (m), 779 (m) cm^{-1}. MS (FAB^+): *m*/*z* 731.1 ([Tb(**L2**)]$^+$, 100%). Anal. Calcd for $C_{33}H_{28}N_6O_4Tb \cdot Cl \cdot 3H_2O$: C, 48.27; H, 4.17; N, 10.24. Found: C, 47.97; H, 3.76; N, 10.01.

Synthesis of [Eu(L3)(H$_2$O)$_2$]Cl·H$_2$O. A solution of $EuCl_3 \cdot 6H_2O$ (9.0 mg, 24 μmol) in MeOH (10 mL) was added to a solution of ligand **L3**H_2 (20.0 mg, 25 μmol) in a mixture of 10 mL of MeOH and 3 mL of H_2O. The resulting mixture was agitated for 16 h at 70 °C. After addition of triethylamine (15 μL, 108 μmol) and an additional 3 h of agitation at room temperature, the solution was concentrated in vacuo. Addition of Et_2O led to the precipitation of the desired complex, which was isolated by centrifugation and dried under vacuum. Yield: 19.1 mg (87%), white crystalline powder. IR (solid): 3361 (s), 2961 (w), 1627 (m), 1596 (s), 1572 (s), 1456 (m), 1372 (m), 1013 (m), 777 (s) cm^{-1}. MS (FAB^+): *m*/*z* 800.2 ([Eu(**L3**)]$^+$, 80%), 802.1 ([Eu(**L3**)]$^+$, 100%). Anal. Calcd for $C_{38}H_{31}ClN_7O_4Eu \cdot 3H_2O$: C, 51.21; H, 4.18; N, 11.00. Found: C, 51.09; H, 4.01; N, 10.73.

Synthesis of [Tb(L3)(H$_2$O)$_2$]Cl·H$_2$O. A solution of $TbCl_3 \cdot 6H_2O$ (9.2 mg, 25 μmol) in MeOH (10 mL) was added to a solution of ligand **13c** (20.0 mg, 25 μmol) in a mixture of 10 mL of MeOH and 3 mL of H_2O. The resulting mixture was agitated for 16 h at 70 °C. After addition of triethylamine (15 μL, 108 μmol) and an additional 3 h of agitation at room temperature, the solution was concentrated in vacuo. Addition of Et_2O led to the precipitation of the desired complex, which was isolated by centrifugation and dried under vacuum. Yield: 17.8 mg (81%), orange crystalline solid. IR (solid): 3346 (s), 2962 (w), 1628 (m), 1596 (s), 1571 (s), 1455 (m), 1368 (m), 1014 (m), 776 (s) cm^{-1}. MS (FAB^+): *m*/*z* 808.1 ([Tb(**L3**)]$^+$, 85%). Anal. Calcd for $C_{38}H_{31}ClN_7O_4Tb \cdot 3H_2O$: C, 50.82; H, 4.15; N, 10.92. Found: C, 50.62; H, 3.86; N, 10.76.

Acknowledgment. This work was supported by the French Centre National de la Recherche Scientifique, the University Louis Pasteur of Strasbourg, and the European Community (IST/ILO Contract 2001-33057). We are indebted to the Centro de Supercomputación de Galicia for providing the computer facilities. The support and sponsorship arranged by the EU COST Action D38 "Metal-Based Systems for Molecular Imaging Applications" is also kindly acknowledged.

Supporting Information Available: Figures giving absorption and emission spectra of the complexes, ^1H NMR spectra of the ligands, spectrophotometric titrations of the complexes, and tables giving intensity decay fitting procedures and optimized Cartesian coordinates of the [Eu(**L***X*′)(H$_2$O)$_2$]$^+$ complexes (*X* = 1−3) in vacuo and in water and of [Eu(**L2**′)(MeTP)]$^{3-}$ and [Eu(**L2**′)(MeTP)(H$_2$O)]$^{3-}$ in vacuo. This material is available free of charge via the Internet at http://pubs.acs.org.

IC702472N